

A study on the reference frame consistency in recent Earth gravitational models

Christopher Kotsakis

Received: 17 April 2007 / Accepted: 28 March 2008 / Published online: 25 April 2008
© Springer-Verlag 2008

Abstract All gravity field functionals obtained from an Earth gravitational model (EGM) depend on the underlying terrestrial reference frame (TRF), with respect to which the EGM's spherical harmonic coefficients refer to. In order to maintain a coherent framework for the comparison of current and future EGMs, it is thus important to investigate the consistency of their inherent TRFs, especially when their use is intended for high precision studies. Following the methodology described in an earlier paper by Kleusberg (1980), the similarity transformation parameters between the associated reference frames for several EGMs (including the most recent CHAMP/GRACE models at the time of writing this paper) are estimated in the present study. Specifically, the differences between the spherical harmonic coefficients for various pairs of EGMs are parameterized through a 3D-similarity spatial transformation model that relates their underlying TRFs. From the least-squares adjustment of such a parametric model, the origin, orientation and scale stability between the EGMs' reference frames can be identified by estimating their corresponding translation, rotation and scale factor parameters. Various aspects of the estimation procedure and its results are highlighted in the paper, including data weighting schemes, the sensitivity of the results with respect to the selected harmonic spectral band, the correlation structure and precision level of the estimated transformation parameters, the effect of the estimated differences of the EGMs' reference frames on their height anomaly signal, and the overall feasibility of Kleusberg's formulae for the assessment of TRF inconsistencies among global geopotential models.

Keywords Earth gravitational models · GRACE · CHAMP · Reference frame · Spherical harmonics · Similarity transformation

1 Introduction

During the last 5 years, and after the launch of the CHAMP and GRACE satellite missions, more than 20 new spherical harmonic models have become available for Earth's static gravitational field. These developments represent the culmination in modern global gravity field mapping after the breakthrough release of the *EGM96* model (Lemoine et al. 1998), involving new types of satellite-borne measurements that have been analyzed by a variety of mathematical models and data processing techniques (e.g. Ditmar et al. 2006; Földvay et al. 2005; Gerlach et al. 2003; Ilk et al. 2005; Mayer-Gürr et al. 2005; Reigber et al. 2002, 2003a,b, 2005). Several combined Earth gravitational models (EGMs) based on CHAMP and/or GRACE satellite data, complete to spherical harmonic degree and order 360, have been produced using additional information from terrestrial gravimetry and satellite altimetry (Förste et al. 2006; Reigber et al. 2006; Tapley et al. 2005), which can recover regional spatial features up to ~110 km resolution in the geoid and gravity anomaly signals at an average accuracy level of ~30 cm and ~8 mgal, respectively (Förste et al. 2005).

In view of the increasing need to compare different EGMs and to evaluate their accuracy for various gravity field functionals, it is important to investigate the consistency of their inherent reference frames. Each EGM given in terms of a set of spherical harmonic coefficients (SHCs) underlies a specific terrestrial reference frame (TRF) which should be used for all SHC-based gravity field calculations with the particular model. Such a TRF is usually realized through an appropriate

C. Kotsakis (✉)
Department of Geodesy and Surveying,
Aristotle University of Thessaloniki,
University Box 440, Thessaloniki 54124, Greece
e-mail: kotsaki@topo.auth.gr

set of constraints that are applied to a number of terrestrial stations for the purpose of removing the rank deficiency of the satellite tracking data that lead to the estimation of the low-degree SHCs (Pavlis 1998). This option is followed when a simultaneous solution for the tracking station positions (and possibly velocities) along with the geopotential coefficients is sought, as it was done, for example, in the case of *EGM96* (Lemoine et al. 1998). Alternatively, one may adopt an existing global TRF to fix a priori the EGM's reference frame, and then process the tracking data (along with other types of gravity field observables coming from dedicated satellite gravity missions such as GRACE and CHAMP) exclusively for geopotential recovery.

Several investigations exist in the geodetic literature that have dealt with TRF consistency issues in global geopotential models (Anderle 1974; Rapp and Rummel 1976; Schaab and Groten 1979; Grappo 1980; Lachapelle and Kouba 1981; Weigel 1993; Kirby and Featherstone 1997; Pavlis 1998). Despite the varying interpretations of their results, most of these studies have relied on a common methodology, notably the comparison of geometrically derived and EGM-based geoid undulations over a global, continental or regional network of control stations. Using the general model

$$h - H - N^{EGM} = N_0 + N_1 \quad (1)$$

the zero- and first-degree geoidal terms, N_0 and N_1 , can be estimated through a least-squares adjustment of pointwise geoid undulation differences obtained from GPS data (or from Doppler measurements in earlier studies), spirit-leveled orthometric heights, and a SHC model of Earth's gravitational field. Equation (1) has been used for the comparison of geoid undulations (and their inherent TRFs) obtained from different EGMs (Schaab and Groten 1979), as well as for the assessment of the TRF consistency between altimetrically derived geoids and EGM-based geoid models (e.g. West 1982; Engelis 1985).

In principle, the zero-degree term N_0 contains the effects of the mass and potential differences between the 'true' geoid and the reference equipotential ellipsoid implied in the determination of N^{EGM} (Heiskanen and Moritz 1967, p. 101)

$$N_0 = \frac{G\delta M}{r\gamma} - \frac{\delta W}{\gamma} \quad (2)$$

and it will appear as a constant offset between the geometric and the EGM geoid heights. Since the term $\delta W = W_0 - U_0$ depends on a conventional choice for the normal gravity potential of the reference ellipsoid and the selection of the particular equipotential surface of Earth's gravity field ($W = W_0$) representing the geoid, the physical meaning of the zero-degree term in Eq. (1) is mainly hidden in our insufficient knowledge of the real Earth's mass.

In practice, the estimate of N_0 that is obtained from the joint adjustment of ellipsoidal, orthometric and geoid heights

absorbs additional systematic effects originating from: (1) the offset between the vertical datum implicated in the calculation of H and the reference equipotential surface associated with N^{EGM} , and (2) the possible differences in the defining parameters of the adopted reference ellipsoids for the geometric and the EGM geoid. Other biases due to datum scale differences (Soler and van Gelder 1987; Kotsakis 2008) and the inconsistent treatment of permanent tidal effects (Smith 1998; Vatr 1999; McCarthy and Petit 2004) may additionally contribute to the final estimate of N_0 .

The first-degree term in Eq. (1) stems from the spatial offset between the TRFs involved in the determination of h and N^{EGM} . While the TRF of the geometric geoid is dictated by the GPS heights that appear in Eq. (1), the TRF of N^{EGM} depends on the conventions and constraints that were used in the development of the underlying EGM. Using the well known geoid transformation due to a datum shift (Heiskanen and Moritz 1967, p. 99)

$$\delta N (= N_1) = t_x \cos\varphi \cos\lambda + t_y \cos\varphi \sin\lambda + t_z \sin\varphi \quad (3)$$

the 3D translation parameters t_x , t_y and t_z can be estimated from the least-squares adjustment of Eq. (1). Assuming that the ellipsoidal heights underlying the geometric geoid refer to a geocentric reference system, these parameters provide a geocentricity assessment for the inherent TRF of the geopotential model from which N^{EGM} is computed (e.g. Rapp and Rummel 1976; Grappo 1980; Weigel 1993).

Based on the above approach, the corresponding corrections to the zero- and first-degree SHCs for a number of known EGMs have been determined by Kirby and Featherstone (1997), using GPS and spirit-leveled heights over Australia. Also, Schaab and Groten (1979) applied the least-squares fitting of Eq. (1) to globally and uniformly distributed geoid undulations obtained from different geopotential models, thus providing a direct comparison of their TRFs' origins without relying on GPS/Doppler satellite data and spirit-leveled orthometric heights.

A drawback of the aforementioned methodology is that the TRF translation parameters obtained from the inversion of Eq. (1) are inevitably distorted due to the high correlation caused by the non-uniform distribution and limited spatial coverage of the control points. Even in cases with a truly global and uniform distribution of data points (Schaab and Groten 1979), the conclusions drawn from such an evaluation scheme are likely to be obscured by the coupling of several long-wavelength data biases into the zero- and first-degree geoidal terms N_0 and N_1 ; see Weigel (1993).

Orientation differences between the EGMs' reference frames can also affect the comparison and/or combination of gravity field functionals obtained from their SHCs. It should be noted that the geoid height is totally insensitive to the rotation of the underlying TRF about the symmetry axis of

the adopted reference ellipsoid, and it is thus impossible to estimate this datum transformation parameter solely from the residuals $h - H - N^{EGM}$. The latter are able to recover only variations in the direction of the mean Earth rotation axis that is implied in the geometric and EGM geoids, and not orientation differences in the zero-meridian planes of their associated TRFs.

Following the above remarks, the objective of this paper is to implement an alternative approach for TRF consistency testing in EGMs, using a different framework than the ‘indirect’ methodologies which are based on Eq. (1). In particular, the formulation given in Kleusberg (1980) on the similarity transformation of a SHC series is employed for the estimation of origin, orientation and scale variations among the TRFs implied in recent static EGMs. The benefit of such an approach is that it does not involve the intermediate computation and comparison of other gravity field functionals, but it relies entirely on the original SHCs for Earth’s gravitational potential. The similarity transformation parameters between the inherent TRFs in geopotential models are fully estimable from the differences of their corresponding SHCs (Kleusberg 1980), and this is exactly the qualitative property that will be numerically investigated in this paper.

Using the aforementioned approach, the problems that commonly arise from Eq. (1) due to the joint analysis of several heterogeneous data types, each of which carries its own reference frame, modeling assumptions and systematic errors, are largely avoided. The mathematical model that is now used for comparing geodetic reference frames has an intrinsic ‘global’ geometric character with uniform spatial resolution (more details to be given in later sections), and thus all the estimated TRF transformation parameters are practically uncorrelated, without being affected by network geometry or spatial coverage problems. Furthermore, the stability of the terrestrial zero-meridian plane among different geopotential models (which is equivalent to a rotation of the EGM-linked TRFs about the symmetry axis of an adopted reference ellipsoid) is now estimable from the differences of their non-zonal SHCs. This ‘z-axis’ rotation angle, however, remains the most weakly estimable transformation parameter between the EGMs’ reference frames, as it will be confirmed by our results.

The paper is organized as follows: in Sect. 2 a general overview of Kleusberg’s (1980) transformation model is given without its detailed mathematical proof, but with some additional corrections and theoretical explanations; in Sect. 3 the least-squares estimation procedure and some data weighting aspects that were followed for the numerical tests of the paper are described; in Sect. 4 a series of numerical tests that have been performed with Kleusberg’s (1980) transformation model is presented, while in Sect. 5 the main conclusions and a short discussion of our findings are given.

2 Reference frame transformation of a SHC series

The earliest studies on the problem of transforming a SHC series under arbitrary translations, rotations and scale change of its underlying Cartesian coordinate system should be attributed to Schmidt (1899), Wigner (1959, Chap. 15) and Jeffreys (1963). The most comprehensive work in the geodetic and geophysical literature is due to Goldstein (1984), who presented an in-depth analysis for the nonlinear effect of reference system rotations on the transformed values of the geopotential SHCs. Equivalent transformation formulae have also been derived by Balmino and Borderies (1976) and Shkodrov (1981), whereas relevant studies related to applications in satellite geodesy, potential field theory and spatial correlation analysis have been published by Kaula (1961), Cook (1963), Izsak (1964), Giacaglia (1980) and Eckhardt (1984).

Our present study is based on the mathematical work of Kleusberg (1980), who presented a linear approximation scheme for the transformation properties of the gravitational potential SHCs due to translation, rotation and scale variation in their underlying TRF. Although the linearized formulae derived in that study are theoretically less rigorous than other versions that appeared in previous references (e.g. Goldstein 1984), they are fairly precise for practical use in geodetic studies where small (differential) TRF perturbations are commonly involved (Pavlis 1998). Moreover, the complexity of the nonlinear transformation equations, in conjunction with their increasing numerical instability in high-degree SHC series expansions, can cause considerable problems in their forward implementation (with known transformation parameters) or in their optimal inversion (with unknown transformation parameters).

2.1 General remarks

The usual expansion of Earth’s gravitational potential in terms of a SHC series is

$$V(r, \lambda, \varphi) = \frac{GM}{r} \sum_{n=0}^{\infty} \left(\frac{a}{r}\right)^n \times \sum_{m=0}^n [\bar{C}_{nm} \cos m\lambda + \bar{S}_{nm} \sin m\lambda] \bar{P}_{nm}(\sin\varphi) \tag{4}$$

where r, λ, φ denote the spherical geodetic coordinates (radial distance, geodetic longitude, geocentric latitude) of an arbitrary evaluation point P that is located on, or outside, the Earth’s surface; see Fig. 1. The set $\{\bar{C}_{nm}, \bar{S}_{nm}\}$ contains unitless fully-normalized SHCs which are obtained from a global geopotential model (up to a maximum degree n_{max}), while $\bar{P}_{nm}(\cdot)$ represent the fully-normalized

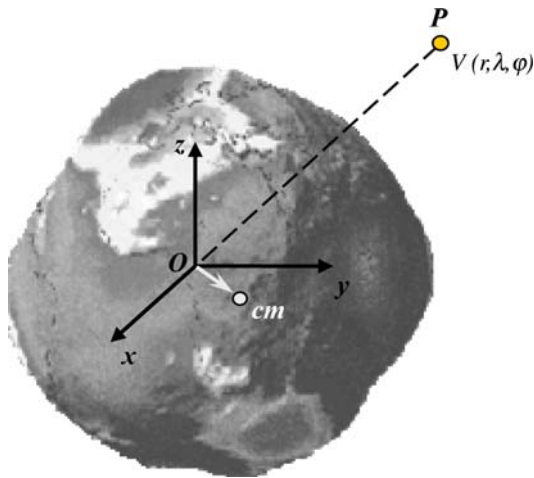


Fig. 1 The TRF associated with the SHC series expansion of Earth’s gravitational potential in Eq. (4) (*cm*: geocenter)

associated Legendre functions of degree n and order m (Heiskanen and Moritz 1967, Chap. 1). The quantities GM and a correspond to the *geocentric gravitational constant* and *mean equatorial radius*, which are the basic Earth-scaling factors that are commonly associated with a geopotential model.

In most EGMs, the zero-degree coefficient $\bar{C}_{0,0}$ is usually treated as an errorless quantity, with its value fixed a priori to 1. Based on Eq. (4), this gives an initial approximation for Earth’s gravitational potential

$$V(r, \lambda, \varphi) \approx \frac{GM}{r} \bar{C}_{0,0} = \frac{GM}{r} \tag{5}$$

which corresponds to a point-mass or a homogeneous-sphere Earth model, with the origin of the inherent TRF located at the geocenter. In essence, the zero-degree coefficient $\bar{C}_{0,0}$ controls the spatial scale of the Euclidean TRF that is associated with an EGM solution and its formally induced (i.e. the TRF’s scale) by the GM value that appears in Eq. (4).

In some geopotential models, the zero-degree coefficient $\bar{C}_{0,0}$ is not conventionally fixed to 1, while its actual value is accompanied by an error estimate $\sigma_{\bar{C}_{0,0}}$ that reflects the uncertainty of the geocentric gravitational ‘constant’. In Table 1, a selected list of global geopotential models that will be used in our tests is given along with their conventional GM values, their original $\bar{C}_{0,0}$ coefficients and their corresponding inferred estimates for GM. From these models, only *TUMIS*, *TUM2S* and *GRIM5C1* are associated with zero-degree SHCs that are not constrained a priori to 1, thus enforcing a theoretically different spatial scale in their underlying TRFs than the one implied by the conventional GM value that appears in Eq. (4). The official error estimates for the zero-degree SHCs of these models are given in Table 2, along with the standard deviations for the inferred values of the geocentric gravitational constant.

Note that the accuracy values shown in Table 2 are quite optimistic with respect to the IERS standard uncertainty of $\sigma_{GM} = 0.8 \times 10^6 \text{ m}^3\text{s}^{-2}$ (McCarthy and Petit 2004), or the formal GM estimation accuracy of $\sigma_{GM} = 0.12 \times 10^6 \text{ m}^3\text{s}^{-2}$ obtained by Pavlis (2002). For practical purposes, the IERS uncertainty level for GM can be used to assign a realistic error variance to the zero-degree coefficient in current ‘scale-fixed’ EGMs, based on the simple formula

$$\sigma_{\bar{C}_{0,0}} = \frac{\sigma_{GM}}{GM} \tag{6}$$

Table 1 GM values associated with various EGMs and their fixed or estimated zero-degree SHC. (GM values are given in $\text{m}^3 \text{s}^{-2}$)

Model	GM (conventional value)	$\bar{C}_{0,0}$	GM (inferred estimate)
<i>EIGEN-CG03C</i>	398600.4415×10^9	1.0000000000000000	Fixed
<i>EIGEN-GL04C</i>	398600.4415×10^9	1.0000000000000000	Fixed
<i>EIGEN-CG01C</i>	398600.4415×10^9	1.0000000000000000	Fixed
<i>EIGEN-CHAMP03S</i>	398600.4415×10^9	1.0000000000000000	Fixed
<i>ITG-GRACE02S</i>	398600.4415×10^9	1.0000000000000000	Fixed
<i>GGM02C</i>	398600.4415×10^9	1.0000000000000000	Fixed
<i>GGM02S</i>	398600.4415×10^9	1.0000000000000000	Fixed
<i>TUM2S</i>	398600.4418×10^9	1.0000000002947140	398600.4419×10^9
<i>TUM1S</i>	398600.4360×10^9	0.9999999996743549	398600.4359×10^9
<i>EIGEN-GRACE02S</i>	398600.4415×10^9	1.0000000000000000	Fixed
<i>EIGEN-GRACE01S</i>	398600.4415×10^9	1.0000000000000000	Fixed
<i>EIGEN2</i>	398600.4415×10^9	1.0000000000000000	Fixed
<i>EIGEN1S</i>	398600.4415×10^9	1.0000000000000000	Fixed
<i>GRIM5C1</i>	398600.4415×10^9	0.9999999998860000	398600.4415×10^9
<i>EGM96</i>	398600.4415×10^9	1.0000000000000000	Fixed

Table 2 Formal uncertainty of the zero-degree SHC and the corresponding standard deviation of the GM inferred estimate, for the *TUMIS*, *TUM2S* and *GRIM5C1* models (GM sigma values are given in m^3s^{-2})

Model	$\sigma_{\bar{C}_{0,0}}$	σ_{GM}
<i>TUM2S</i>	$1.62270320 \times 10^{-11}$	0.006×10^6
<i>TUMIS</i>	$1.97626465 \times 10^{-11}$	0.008×10^6
<i>GRIM5C1</i>	$3.07800000 \times 10^{-11}$	0.012×10^6

In general, the inclusion of $\sigma_{\bar{C}_{0,0}}$ in the evaluation of the total commission error for EGM-based gravity field functionals yields a more rigorous assessment of their actual accuracy, since it incorporates the effect of spatial scale uncertainty of their underlying TRF (Zhu et al. 2001).

The first-degree SHCs $\bar{C}_{1,0}$, $\bar{C}_{1,1}$, $\bar{S}_{1,1}$ are directly related to the offset of the origin of the EGM’s TRF (in which the coordinates r , λ , φ in Eq. (4) should refer to) with respect to the geocenter. In fact, we have the following relationships

$$x_{cm} = \frac{\text{GM}}{\text{GM}_{\text{true}}} a\sqrt{3}\bar{C}_{1,1} \tag{7}$$

$$y_{cm} = \frac{\text{GM}}{\text{GM}_{\text{true}}} a\sqrt{3}\bar{S}_{1,1} \tag{8}$$

$$z_{cm} = \frac{\text{GM}}{\text{GM}_{\text{true}}} a\sqrt{3}\bar{C}_{1,0} \tag{9}$$

where x_{cm} , y_{cm} , z_{cm} are the Cartesian coordinates of the geocenter with respect to the global TRF associated with the SHC series in Eq. (4); see Fig. 1. For more details, see Heiskanen and Moritz (1967, Chap. 2).

Instead of the above ‘theoretical’ equations, the following alternative expressions can also be used

$$x_{cm} = \frac{a\sqrt{3}}{\bar{C}_{0,0}} \bar{C}_{1,1} \tag{10}$$

$$y_{cm} = \frac{a\sqrt{3}}{\bar{C}_{0,0}} \bar{S}_{1,1} \tag{11}$$

$$z_{cm} = \frac{a\sqrt{3}}{\bar{C}_{0,0}} \bar{C}_{1,0} \tag{12}$$

The last three equations establish a link between the spatial scale that is realized by the TRF of a global geopotential model, with its zero-degree coefficient and the adopted Earth’s mean equatorial radius.

In most EGMs, the coefficients $\bar{C}_{1,0}$, $\bar{C}_{1,1}$, $\bar{S}_{1,1}$ are set a priori to zero, thus enforcing a geocentricity constraint for their inherent TRFs. However, in a number of recent CHAMP and GRACE models, non-zero values and associated error variances are given for their first-degree SHCs, which are handled as additional unknown parameters and estimated anew within the EGM development process. The geocenter’s Cartesian coordinates and their formal accuracy level

Table 3 Geocenter’s Cartesian coordinates (and their formal uncertainty level) with respect to the inherent TRFs in GRACE/CHAMP models with non-zero first-degree SHCs (all values are given in mm)

Model	x_{cm}	y_{cm}	z_{cm}
<i>EIGEN-CG03C</i>	-5.5 ± 4.8	-0.3 ± 4.8	-15.2 ± 4.4
<i>EIGEN-CG01C</i>	-3.8 ± 6.1	1.2 ± 6.1	-11.9 ± 5.5
<i>EIGEN-CHAMP03S</i>	-2.7 ± 3.3	0.6 ± 3.3	-9.2 ± 3.4
<i>TUM2S</i>	0.2 ± 0.2	0.7 ± 0.2	0.2 ± 0.2
<i>TUMIS</i>	-1.1 ± 0.2	-2.1 ± 0.2	-15.1 ± 0.2

(as obtained from the last three equations) with respect to the TRFs of these models are given in Table 3.

Note that the error propagation formulae for the assessment of $\sigma_{x_{cm}}$, $\sigma_{y_{cm}}$, and $\sigma_{z_{cm}}$ in EGMs with estimated (i.e. not fixed to zero) first-degree SHCs have the general form

$$\sigma_{x_{cm}}^2 = \left(\frac{a\sqrt{3}}{\bar{C}_{0,0}} \right)^2 \left(\sigma_{\bar{C}_{1,1}}^2 + \bar{C}_{1,1}^2 \sigma_{\bar{C}_{0,0}}^2 \right) \tag{13}$$

$$\sigma_{y_{cm}}^2 = \left(\frac{a\sqrt{3}}{\bar{C}_{0,0}} \right)^2 \left(\sigma_{\bar{S}_{1,1}}^2 + \bar{S}_{1,1}^2 \sigma_{\bar{C}_{0,0}}^2 \right) \tag{14}$$

$$\sigma_{z_{cm}}^2 = \left(\frac{a\sqrt{3}}{\bar{C}_{0,0}} \right)^2 \left(\sigma_{\bar{C}_{1,0}}^2 + \bar{C}_{1,0}^2 \sigma_{\bar{C}_{0,0}}^2 \right) \tag{15}$$

which include the effect of the EGM/TRF’s spatial scale uncertainty (i.e. GM uncertainty) through the error term $\sigma_{\bar{C}_{0,0}}$. The latter can be practically determined from Eq. (6) using the IERS standard uncertainty for GM, or it may formally be provided by the corresponding EGM solution (e.g. *TUMIS*, *TUM2S*).

2.2 Linearized TRF transformation for $\{\bar{C}_{nm}, \bar{S}_{nm}\}$ (Kleusberg 1980)

A brief overview of Kleusberg’s TRF transformation formulae (without their mathematical proof) will be presented in this section, along with some additional corrections that were missing from their original publication.

The expansion of the gravitational potential $V(\cdot)$ in a different Earth-fixed TRF than the one implied in Eq. (4) has the general form

$$V(r', \lambda', \varphi') = \frac{\text{GM}}{r'} \sum_{n=0}^{\infty} \left(\frac{a}{r'} \right)^n \times \sum_{m=0}^n [\bar{C}'_{nm} \cos m\lambda' + \bar{S}'_{nm} \sin m\lambda'] \bar{P}_{nm}(\sin \varphi') \tag{16}$$

where r' , λ' , φ' are the spherical geodetic coordinates of the evaluation point with respect to a new Cartesian coordinate

system $O'x'y'z'$; see Fig. 2. Note that the basic scaling factors of the geopotential SHCs are assumed to retain their conventional values in both frames.

Let us assume that the two TRFs differ according to the linearized similarity (Helmert-type) transformation model (e.g. Leick and van Gelder 1975; Soler 1998)

$$\begin{bmatrix} x' - x \\ y' - y \\ z' - z \end{bmatrix} = \begin{bmatrix} t_x \\ t_y \\ t_z \end{bmatrix} + \begin{bmatrix} \delta s & \varepsilon_z & -\varepsilon_y \\ -\varepsilon_z & \delta s & \varepsilon_x \\ \varepsilon_y & -\varepsilon_x & \delta s \end{bmatrix} \begin{bmatrix} x \\ y \\ z \end{bmatrix} \quad (17)$$

equations were originally given by Kleusberg (1980) and they are expressed as

$$\begin{aligned} \bar{C}'_{nm} - \bar{C}_{nm} &= \delta\bar{C}_{nm}(t_x) + \delta\bar{C}_{nm}(t_y) + \delta\bar{C}_{nm}(t_z) \\ &+ \delta\bar{C}_{nm}(\varepsilon_x) + \delta\bar{C}_{nm}(\varepsilon_y) + \delta\bar{C}_{nm}(\varepsilon_z) + \delta\bar{C}_{nm}(\delta s) \end{aligned} \quad (18)$$

$$\begin{aligned} \bar{S}'_{nm} - \bar{S}_{nm} &= \delta\bar{S}_{nm}(t_x) + \delta\bar{S}_{nm}(t_y) + \delta\bar{S}_{nm}(t_z) \\ &+ \delta\bar{S}_{nm}(\varepsilon_x) + \delta\bar{S}_{nm}(\varepsilon_y) + \delta\bar{S}_{nm}(\varepsilon_z) + \delta\bar{S}_{nm}(\delta s) \end{aligned} \quad (19)$$

where each individual transformation term is analytically given by

$$\delta\bar{C}_{nm}(t_x) = -\sqrt{\frac{2n-1}{2n+1}} \frac{\sqrt{(n-m-1)(n-m)(1+\delta_{0m})}\bar{C}_{n-1,m+1} - \sqrt{(n+m-1)(n+m)(1+\delta_{1m})}\bar{C}_{n-1,m-1}}{2a} t_x \quad (20)$$

$$\delta\bar{C}_{nm}(t_y) = -\sqrt{\frac{2n-1}{2n+1}} \frac{\sqrt{(n-m-1)(n-m)(1+\delta_{0m})}\bar{S}_{n-1,m+1} + \sqrt{(n+m-1)(n+m)(1+\delta_{1m})}\bar{S}_{n-1,m-1}}{2a} t_y \quad (21)$$

$$\delta\bar{C}_{nm}(t_z) = \sqrt{\frac{2n-1}{2n+1}} \frac{\sqrt{(n+m)(n-m)}\bar{C}_{n-1,m}}{a} t_z \quad (22)$$

$$\delta\bar{C}_{nm}(\varepsilon_x) = -\frac{\sqrt{(n-m+1)(n+m)(1+\delta_{1m})}\bar{S}_{n,m-1} + \sqrt{(n+m+1)(n-m)(1+\delta_{0m})}\bar{S}_{n,m+1}}{2} \varepsilon_x \quad (23)$$

$$\delta\bar{C}_{nm}(\varepsilon_y) = -\frac{\sqrt{(n-m+1)(n+m)(1+\delta_{1m})}\bar{C}_{n,m-1} - \sqrt{(n+m+1)(n-m)(1+\delta_{0m})}\bar{C}_{n,m+1}}{2} \varepsilon_y \quad (24)$$

$$\delta\bar{C}_{nm}(\varepsilon_z) = m\bar{S}_{n,m}\varepsilon_z \quad (25)$$

$$\delta\bar{C}_{nm}(\delta s) = (n+1)\bar{C}_{n,m}\delta s \quad (26)$$

$$\delta\bar{S}_{nm}(t_x) = -\sqrt{\frac{2n-1}{2n+1}} \frac{\sqrt{(n-m-1)(n-m)(1+\delta_{0m})}\bar{S}_{n-1,m+1} - \sqrt{(n+m-1)(n+m)(1+\delta_{1m})}\bar{S}_{n-1,m-1}}{2a} t_x \quad (27)$$

$$\delta\bar{S}_{nm}(t_y) = \sqrt{\frac{2n-1}{2n+1}} \frac{\sqrt{(n-m-1)(n-m)(1+\delta_{0m})}\bar{C}_{n-1,m+1} + \sqrt{(n+m-1)(n+m)(1+\delta_{1m})}\bar{C}_{n-1,m-1}}{2a} t_y \quad (28)$$

$$\delta\bar{S}_{nm}(t_z) = \sqrt{\frac{2n-1}{2n+1}} \frac{\sqrt{(n+m)(n-m)}\bar{S}_{n-1,m}}{a} t_z \quad (29)$$

$$\delta\bar{S}_{nm}(\varepsilon_x) = \frac{\sqrt{(n-m+1)(n+m)(1+\delta_{1m})}\bar{C}_{n,m-1} + \sqrt{(n+m+1)(n-m)(1+\delta_{0m})}\bar{C}_{n,m+1}}{2} \varepsilon_x \quad (30)$$

$$\delta\bar{S}_{nm}(\varepsilon_y) = -\frac{\sqrt{(n-m+1)(n+m)(1+\delta_{1m})}\bar{S}_{n,m-1} - \sqrt{(n+m+1)(n-m)(1+\delta_{0m})}\bar{S}_{n,m+1}}{2} \varepsilon_y \quad (31)$$

$$\delta\bar{S}_{nm}(\varepsilon_z) = -m\bar{C}_{n,m}\varepsilon_z \quad (32)$$

$$\delta\bar{S}_{nm}(\delta s) = (n+1)\bar{S}_{n,m}\delta s \quad (33)$$

where t_x, t_y, t_z are the translation parameters between the two frames, $\varepsilon_x, \varepsilon_y, \varepsilon_z$ are the rotation angles about the axes of the $Oxyz$ frame (anti-clockwise rotations assumed positive), and δs is the unitless differential factor of their spatial scale change.

Based on the spatial transformation model of Eq. (17) and the fact that the gravitational potential $V(\cdot)$ is independent of the TRF in which we choose to perform its evaluation through a SHC series, a set of linearized transformation formulae can be derived between $\{\bar{C}_{nm}, \bar{S}_{nm}\}$ and $\{\bar{C}'_{nm}, \bar{S}'_{nm}\}$. These

The terms δ_{0m} and δ_{1m} correspond to the Kronecker delta symbol (e.g. $\delta_{1m} = 1$ when $m = 1$, and $\delta_{1m} = 0$ otherwise). For the detailed proof of the above equations, see Kleusberg (1980).

From the previous TRF/SHC transformation model, the following ‘aliasing’ aspects can be identified:

- *rotational variation about the x axis* causes changes in the \bar{C} -type harmonics of order m that are proportional to

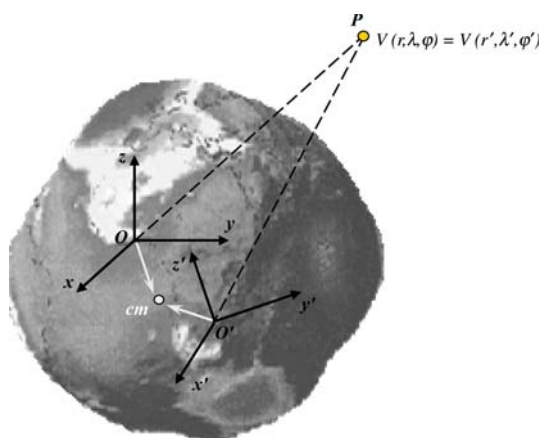


Fig. 2 The TRFs associated with the SHC series expansions of Earth’s gravitational potential in Eqs. (4) and (9) (*cm*: geocenter)

the \bar{S} -type harmonics of order $m - 1$ and $m + 1$, within the same degree; see Eq. (23)

- *rotational variation about the x axis* causes changes in the \bar{S} -type harmonics of order m that are proportional to the \bar{C} -type harmonics of order $m - 1$ and $m + 1$, within the same degree; see Eq. (30)
- *rotational variation about the y axis* causes changes in the \bar{C} -type harmonics of order m that are proportional to the \bar{C} -type harmonics of order $m - 1$ and $m + 1$, within the same degree; see Eq. (24)
- *rotational variation about the y axis* causes changes in the \bar{S} -type harmonics of order m that are proportional to the \bar{S} -type harmonics of order $m - 1$ and $m + 1$, within the same degree; see Eq. (31)
- *rotational variation about the z axis* causes change in the \bar{C} -type harmonics of degree n and order m that are proportional to the \bar{S} -type harmonics of the same degree and order; see Eq. (25)
- *rotational variation about the z axis* causes changes in the \bar{S} -type harmonics of degree n and order m that are proportional to the \bar{C} -type harmonics of the same degree and order; see Eq. (32)
- *translation along the x axis* causes changes in the \bar{C} -type harmonics of degree n and order m that are proportional to the \bar{C} -type harmonics of the previous degree ($n - 1$) and order $m - 1$ and $m + 1$; see Eq. (20)
- *translation along the x axis* causes changes in the \bar{S} -type harmonics of degree n and order m that are proportional to the \bar{S} -type harmonics of the previous degree ($n - 1$) and order $m - 1$ and $m + 1$; see Eq. (27)
- *translation along the y axis* causes changes in the \bar{C} -type harmonics of degree n and order m that are proportional to the \bar{S} -type harmonics of the previous degree ($n - 1$) and order $m - 1$ and $m + 1$; see Eq. (21)
- *translation along the y axis* causes changes in the \bar{S} -type harmonics of degree n and order m that are proportional

to the \bar{C} -type harmonics of the previous degree ($n - 1$) and order $m - 1$ and $m + 1$; see Eq. (28)

- *translation along the z axis* causes changes in the \bar{C} -type harmonics of degree n and order m that are proportional to the \bar{C} -type harmonics of degree $n - 1$, within the same order; see Eq. (22)
- *translation along the z axis* causes changes in the \bar{S} -type harmonics of degree n and order m that are proportional to the \bar{S} -type harmonics of degree $n - 1$, within the same order; see Eq. (29)
- *spatial scale variation* causes changes in each harmonic by a degree-dependent linear scaling factor (assuming that the GM and a values remain unaffected by the TRF transformation); see Eqs. (26) and (33).

Note that the term $(1 + \delta_{0m})$ that appears in the definition of the transformation components $\delta\bar{C}_{nm}(t_x)$, $\delta\bar{C}_{nm}(t_y)$, $\delta\bar{S}_{nm}(t_x)$, $\delta\bar{S}_{nm}(t_y)$, $\delta\bar{C}_{nm}(\varepsilon_x)$, $\delta\bar{C}_{nm}(\varepsilon_y)$, $\delta\bar{S}_{nm}(\varepsilon_x)$ and $\delta\bar{S}_{nm}(\varepsilon_y)$ was missing from the original formulae given in Kleusberg (1980), probably due to an incorrect implementation of the non-normalized to fully-normalized SHC transformation (*ibid*, sect. 3). The inclusion of this term is necessary in order to maintain correct transformation results for the zonal harmonic coefficients.

Depending on the particular values for the harmonic degree and order of the coefficient \bar{C}_{nm} or \bar{S}_{nm} that is being transformed, algebraic terms containing ‘meaningless’ SHCs of the form $\bar{C}_{-1,m+1}$, $\bar{S}_{-1,m+1}$, $\bar{C}_{n-1,-1}$, $\bar{S}_{n-1,-1}$, $\bar{C}_{n,-1}$, $\bar{S}_{n,-1}$, $\bar{C}_{-1,m}$, $\bar{S}_{-1,m}$, $\bar{C}_{n-1,n}$, $\bar{S}_{n-1,n}$, $\bar{C}_{n-1,n+1}$ and $\bar{S}_{n-1,n+1}$ may appear at the right hand-side of Eqs. (18) and (19). In such cases, these meaningless SHCs must be set equal to zero for the proper numerical implementation of the entire $\{\bar{C}_{nm}, \bar{S}_{nm}\} \rightarrow \{\bar{C}'_{nm}, \bar{S}'_{nm}\}$ transformation algorithm (*ibid*, appendix).

In summary, Kleusberg’s model can be used for the forward transformation of the geopotential SHCs from their original TRF to another global TRF, based on known values for the similarity transformation parameters between the two frames. Alternatively, Kleusberg’s model may also be implemented in an inverse manner for estimating the TRF discrepancies between different EGMs, based on the adjustment of the differences of their corresponding SHCs (more details are given in following sections).

2.3 ‘Scaling’ issues

Available geopotential models are not always compatible with the same Earth-scaling factors (GM, a). If we want to evaluate the consistency of the inherent TRFs in different EGMs through a least-squares adjustment with Kleusberg’s model, we may need to re-scale their SHCs so that they refer to the same conventional values of GM and a .

Table 4 Conventional values for the Earth-scaling factors associated with the EGMs that are used for the numerical tests in this paper

Model	GM (in m^3s^{-2})	a (in m)	n_{max}
<i>EIGEN-CG03C</i>	398600.4415×10^9	6378136.460	360
<i>EIGEN-GL04C</i>	398600.4415×10^9	6378136.460	360
<i>EIGEN-CG01C</i>	398600.4415×10^9	6378136.460	360
<i>EIGEN-CHAMP03S</i>	398600.4415×10^9	6378136.460	140
<i>ITG-GRACE02S</i>	398600.4415×10^9	6378136.300	170
<i>GGM02C</i>	398600.4415×10^9	6378136.300	200
<i>GGM02S</i>	398600.4415×10^9	6378136.300	160
<i>TUM2S</i>	398600.4418×10^9	6378137.000	60
<i>TUM1S</i>	398600.4360×10^9	6378137.000	60
<i>EIGEN-GRACE02S</i>	398600.4415×10^9	6378136.460	150
<i>EIGEN-GRACE01S</i>	398600.4415×10^9	6378136.460	140
<i>EIGEN2</i>	398600.4415×10^9	6378136.460	140
<i>EIGEN1S</i>	398600.4415×10^9	6378136.460	119
<i>GRIM5C1</i>	398600.4415×10^9	6378136.460	120
<i>EGM96</i>	398600.4415×10^9	6378136.300	360

Assuming that a couple of EGMs with given SHCs $\{\bar{C}_{nm}, \bar{S}_{nm}\}$ and $\{\bar{C}'_{nm}, \bar{S}'_{nm}\}$ need to be tested for their TRF consistency on the basis of Kleusberg's model, the aforementioned re-scaling has the form (Pavlis 1998; Lemoine et al. 1998, Chap. 7, p. 79)

$$\begin{Bmatrix} \bar{C}''_{nm} \\ \bar{S}''_{nm} \end{Bmatrix} = \frac{\text{GM}'}{\text{GM}} \left(\frac{a'}{a}\right)^n \begin{Bmatrix} \bar{C}'_{nm} \\ \bar{S}'_{nm} \end{Bmatrix} \quad (34)$$

where GM' and a' are the scaling factors associated with the original SHCs $\{\bar{C}'_{nm}, \bar{S}'_{nm}\}$ of the second model. The coefficients $\{\bar{C}''_{nm}, \bar{S}''_{nm}\}$ obtained from Eq. (34) are compatible with the values GM and a of the first model $\{\bar{C}_{nm}, \bar{S}_{nm}\}$ and they should be used, instead of $\{\bar{C}'_{nm}, \bar{S}'_{nm}\}$, in the formulation of Kleusberg's transformation equations (which actually require in advance that both sets of SHCs should refer to the same conventional scaling factors). A list with the formal GM and a values associated with the EGMs that will be used in our numerical tests is given in Table 4.

Note that the scale-change parameter (δs) that is estimated through the inversion of Kleusberg's model will be affected by the differences that may originally exist in the formal GM and/or a values of the underling EGMs. This particular transformation parameter will also reflect the combined effect of systematic errors, data biases, and other types of modeling uncertainties that have affected the SHCs of both geopotential models and cause an apparent scale perturbation in their inherent TRFs.

It should be underlined that the scale-dependent variation terms $\delta\bar{C}_{nm}(\delta s)$ and $\delta\bar{S}_{nm}(\delta s)$, during the *forward transformation* of an EGM from its original TRF to another, could be simply replaced by an appropriate re-scaling of the GM

and a values that will accompany the transformed SHCs in the new frame, according to the equations

$$\text{GM}' = (1 + \delta s)\text{GM} \quad (35a)$$

$$a' = (1 + \delta s)a \quad (35b)$$

3 Least-squares estimation procedure

Based on Kleusberg's model, a least-squares adjustment can be performed for the estimation of the similarity transformation parameters between the inherent TRFs in different EGMs. Using matrix notation, the following linear system of observation equations is formed

$$\mathbf{y} = \mathbf{A}\mathbf{x} + \mathbf{v} \quad (36)$$

where \mathbf{y} contains the SHC differences $\bar{C}'_{nm} - \bar{C}_{nm}$ and $\bar{S}'_{nm} - \bar{S}_{nm}$ (or $\bar{C}''_{nm} - \bar{C}_{nm}$ and $\bar{S}''_{nm} - \bar{S}_{nm}$, in case the re-scaling of Eq. (34) is needed), \mathbf{x} is the unknown vector of the TRF transformation parameters, and \mathbf{v} includes the remaining residuals due to non-datum related effects and other errors in the original SHCs. The elements of the design matrix \mathbf{A} are computed through the analytic expressions in Eqs. (20)–(33), taking into account also the remark given in Sect. 2.2 on the appearance of 'meaningless' SHCs in Kleusberg's transformation equations.

Due to the significant differences in the accuracy level of the SHCs within each EGM, a suitable weight matrix \mathbf{P} should be employed for the least-squares adjustment of Eq. (36). For our tests, a diagonal weight matrix has been used, with elements

$$p_i = \frac{1}{\sigma_{\bar{C}'_{nm}}^2 + \sigma_{\bar{C}_{nm}}^2} \quad \text{for each observation of type } \bar{C}'_{nm} - \bar{C}_{nm} \quad (37)$$

and

$$p_i = \frac{1}{\sigma_{\bar{S}'_{nm}}^2 + \sigma_{\bar{S}_{nm}}^2} \quad \text{for each observation of type } \bar{S}'_{nm} - \bar{S}_{nm} \quad (38)$$

where $\sigma_{\bar{C}'_{nm}}^2$, $\sigma_{\bar{C}_{nm}}^2$, $\sigma_{\bar{S}'_{nm}}^2$ and $\sigma_{\bar{S}_{nm}}^2$ are the SHC error variances associated with the corresponding models.

A total of 15 EGMs have been used for our numerical tests (see Table 4). Their SHCs and their error variances have been obtained from the website of the International Centre of Global Earth Models (ICGEM) at the GeoForschungsZentrum (GFZ), Potsdam (<http://icgem.gfz-potsdam.de/ICGEM/ICGEM.html>). In cases where both formal and calibrated error variances are provided for a particular EGM (e.g. *EIGEN-GRACE02S*), the latter have been selected for the statistical weight determination according to Eqs. (37) and (38).

Remark 1 In cases where the SHC re-scaling of Eq. (34) is required, the initial error variances $\sigma_{\bar{C}_{nm}}^2$ and $\sigma_{\bar{S}_{nm}}^2$ of the tested EGM have been accordingly re-scaled before the weight determination.

The geopotential model *EIGEN-CG03C* is adopted as the ‘reference’ model that will be linked to the $\{\bar{C}_{nm}, \bar{S}_{nm}\}$ coefficients in Kleusberg’s formulae. For each adjustment scenario that will be studied, the estimated transformation parameters are always consistent with the scheme *GRF1* → *GRF2*, where *GRF1* is the reference frame of the *EIGEN-CG03C* model, and *GRF2* is the reference frame of every other EGM that is tested. Hence, the values $\{\bar{C}_{nm}, \bar{S}_{nm}\}$ for computing the observation vector \mathbf{y} always correspond to the original SHCs of *EIGEN-CG03C*, whereas the values $\{\bar{C}'_{nm}, \bar{S}'_{nm}\}$ are obtained by applying the re-scaling formula of Eq. (34) to the original SHCs of every other EGM to be tested. Based on our selected EGMs (see Table 4) such a re-scaling is necessary for the models *ITG-GRACE02S*, *GGM02C*, *GGM02S*, *TUM1S*, *TUM2S* and *EGM96*.

Remark 2 The EGMs considered in this paper are all static geopotential models. For some of them, however, time-dependent low-degree zonal SHCs are formally given in terms of their values at a specific epoch and their corresponding ‘velocities’ (i.e. $\bar{C}_{2,0}, \dot{\bar{C}}_{2,0}, \bar{C}_{3,0}, \dot{\bar{C}}_{3,0}, \bar{C}_{4,0}, \dot{\bar{C}}_{4,0}$). In all such cases, the time-dependent SHCs (including the $\bar{C}_{2,0}$ coefficient of *EGM96*) have been transformed to a common reference epoch, $t = 2006.0$, for our following tests.

Remark 3 The second-degree zonal coefficient ($\bar{C}_{2,0}$) in all tested models is expressed in the tide-free system. In cases where the zero-tide system was formally used for some models (*ITG-GRACE02S*, *GGM02C*, *GGM02S*), the following simplified conversion formula has been applied (e.g. Melbourne 1983)

$$\bar{C}_{2,0}^{\text{tide free}} = \bar{C}_{2,0}^{\text{zero tide}} + k \times (1.39 \times 10^{-8})$$

where the zero frequency Love number k has been set to the conventional value 0.3; see also Ekman (1989), Rapp (1989) and Lemoine et al. (1998, Chap. 11).

4 Numerical results

4.1 Using $\{\bar{C}_{nm}, \bar{S}_{nm}\}$ and $\{\bar{C}'_{nm}, \bar{S}'_{nm}\}$ for $n \geq 2$

A first series of least-squares adjustment tests with Kleusberg’s model was performed by using as ‘observations’ the SHC differences $\bar{C}'_{nm} - \bar{C}_{nm}$ and $\bar{S}'_{nm} - \bar{S}_{nm}$ for $n \geq 2$. The differences between the zero- and first-degree harmonic coefficients, as well as their inherent uncertainty (either due to their formal error variances or due to some standard

GM-uncertainty and EGM/geocentricity-uncertainty level) were not taken into account for these preliminary tests.

In all cases, the SHC differences up to maximum degree $n_{max} = 70$ were considered, although the sensitivity of the harmonic coefficients of the gravitational potential with respect to their underlying TRF is mostly limited to a lower-degree spectral band (Pavlis 1998); see also the sensitivity analysis in Sect. 4.4. The only exceptions are the tests performed with *TUM1S* and *TUM2S*, where $n_{max} = 60$ was used due to the limited resolution of these particular models.

The results for the translation, rotation and scale variation parameters are shown in Tables 5, 6 and 7, respectively. An example of the produced correlation matrix for the TRF transformation parameters is given in Table 8, from which we see that the correlation coefficients among all estimated parameters are nearly negligible. This is actually expected due to the fact that Kleusberg’s model inflicts a ‘global spatial coverage’ of TRF information for the recovery of the similarity transformation parameters. Analogous correlation patterns have been obtained in all adjustment tests that have been performed in the present and subsequent sections.

From the results given in Tables 5, 6, 7, the following comments can be made:

- the translation parameters are unrealistically large due to the exclusion of the first-degree SHC differences from the least-squares adjustment of Kleusberg’s model. In particular, the origins of the TRFs in many of the tested EGMs show an estimated offset from a few centimeters upto a few meters, with respect to the origin of *EIGEN-CG03C*. These results essentially reflect the effect of various systematic errors that exist in the EGMs’ harmonic coefficients (for $n \geq 2$), which are ‘mapped’ to a significant (apparent) origin inconsistency between their associated TRFs;
- the rotation about the mean Earth rotation axis (ε_z) is 1–3 orders of magnitude consistently larger than the other two rotation angles ($\varepsilon_x, \varepsilon_y$), with values that reach up to a few arcsec! This may suggest that some inconsistencies possibly exist on the constraints that have been applied for the realization of the terrestrial zero-meridian plane within the EGMs’ reference frames;
- the large uncertainty of ε_z , compared to the estimation accuracy for ε_x and ε_y , indicates the weakness for estimating this particular parameter from the non-zonal SHC differences. Since both sets $\{\bar{C}_{nm}, \bar{S}_{nm}\}, \{\bar{C}'_{nm}, \bar{S}'_{nm}\}$ refer to a global gravitational field with rather small deviations from rotational symmetry, the sensitivity of the SHCs with respect to the rotation angle ε_z becomes much weaker compared to the influence of the ‘equatorial’ rotation angles ε_x and ε_y . Nevertheless, it is evident from Table 6 that the TRFs in many of the tested EGMs are

Table 5 Translation parameters of the inherent TRFs in various EGMs, which are obtained from the least-squares adjustment of Kleusberg's transformation model (with respect to *EIGEN-CG03C*)

Model	Without taking into account zero- and first-degree SHC differences			Taking into account first-degree SHC differences ^a		
	t_x (mm)	t_y (mm)	t_z (mm)	t_x (mm)	t_y (mm)	t_z (mm)
<i>EIGEN-GL04C</i>	98.3 ± 84.2	-63.5 ± 84.3	155.4 ± 46.5	5.7 ± 3.7	0.2 ± 3.7	16.0 ± 3.4
<i>EIGEN-CG01C</i>	56.4 ± 67.8	73.0 ± 68.0	66.4 ± 46.1	2.1 ± 6.0	2.1 ± 6.0	4.2 ± 5.5
<i>EIGEN-CHAMP03S</i>	-27.8 ± 506.2	272.4 ± 507.8	-1449.4 ± 524.6	2.7 ± 9.4	1.0 ± 9.3	5.6 ± 8.8
<i>ITG-GRACE02S</i>	46.2 ± 59.7	-16.1 ± 60.0	408.8 ± 39.6	5.9 ± 6.2	0.2 ± 6.1	22.7 ± 5.5
<i>GGM02C</i>	-45.2 ± 167.8	139.0 ± 168.7	314.4 ± 97.5	5.4 ± 7.3	0.6 ± 7.3	16.6 ± 6.6
<i>GGM02S</i>	-32.6 ± 166.3	152.7 ± 167.1	295.7 ± 96.6	5.4 ± 7.2	0.6 ± 7.2	16.5 ± 6.5
<i>TUM2S</i> ^b	50.5 ± 375.0	-277.5 ± 386.6	188.1 ± 287.1	5.7 ± 14.6	0.7 ± 14.6	15.8 ± 13.2
<i>TUM1S</i> ^b	-89.2 ± 390.8	651.2 ± 401.1	-525.9 ± 303.7	4.3 ± 12.8	-1.1 ± 12.7	-0.6 ± 11.5
<i>EIGEN-GRACE02S</i>	45.5 ± 62.8	74.5 ± 63.4	-98.9 ± 41.1	5.7 ± 4.9	1.3 ± 7.3	13.9 ± 4.4
<i>EIGEN-GRACE01S</i>	141.7 ± 245.1	238.3 ± 246.6	442.8 ± 168.8	5.5 ± 3.6	0.5 ± 5.4	15.4 ± 3.2
<i>EIGEN2</i>	-455.2 ± 127.7	230.2 ± 128.0	-2498.3 ± 131.0	4.5 ± 6.0	0.8 ± 5.9	11.3 ± 5.4
<i>EIGEN1S</i>	-627.6 ± 2549.0	-271.7 ± 2368.7	-2651.0 ± 3691.3	5.5 ± 9.1	0.3 ± 9.0	15.2 ± 8.2
<i>GRIM5C1</i>	916.2 ± 476.1	389.4 ± 437.0	-7098.9 ± 891.2	9.4 ± 31.4	2.3 ± 31.2	8.2 ± 28.3
<i>EGM96</i>	2982.5 ± 1640.9	-1909.5 ± 1615.6	-42.9 ± 182.6	5.6 ± 9.0	0.3 ± 8.9	15.1 ± 8.1

The differences of SHCs with their error variances up to $n_{\max} = 70$ have been used

^a The *first-degree* SHCs of the reference model *EIGEN-CG03C* and of the tested models *EIGEN-CG01C*, *EIGEN-CHAMP03S*, *TUM2S* and *TUM1S*, have been weighted according to the formal error estimates provided by the corresponding models. The (set-to-zero) *first-degree* SHCs of the tested models *EIGEN-GL04C*, *EIGEN-GRACE02S*, *EIGEN-GRACE01S*, *ITG-GRACE02S*, *GGM02C*, *GGM02S*, *EIGEN2*, *EIGEN1S*, *GRIM5C1* and *EGM96*, have been assumed errorless

^b The SHCs with their error variances up to $n_{\max} = 60$ have been used for testing these models

Table 6 Rotation angles of the inherent TRFs in various EGMs, which are obtained from the least-squares adjustment of Kleusberg's transformation model (with respect to *EIGEN-CG03C*)

Model	Without taking into account zero- and first-degree SHC differences			Taking into account first-degree SHC differences ^a		
	ε_x (mas)	ε_y (mas)	ε_z (mas)	ε_x (mas)	ε_y (mas)	ε_z (mas)
<i>EIGEN-GL04C</i>	5.07 ± 3.75	-0.79 ± 3.72	-69.02 ± 53.35	5.04 ± 3.75	-0.88 ± 3.73	-71.05 ± 53.35
<i>EIGEN-CG01C</i>	-0.64 ± 4.11	-2.77 ± 4.09	92.46 ± 61.46	-0.67 ± 4.11	-2.82 ± 4.09	95.20 ± 61.38
<i>EIGEN-CHAMP03S</i>	16.06 ± 22.15	20.18 ± 22.00	-593.11 ± 356.74	15.97 ± 22.16	20.53 ± 22.01	-582.90 ± 356.75
<i>ITG-GRACE02S</i>	-3.98 ± 4.41	-6.43 ± 4.40	-80.90 ± 64.33	-4.02 ± 4.45	-6.97 ± 4.44	-86.01 ± 64.81
<i>GGM02C</i>	17.86 ± 11.50	11.18 ± 11.11	93.64 ± 202.77	17.82 ± 11.51	10.71 ± 11.12	102.93 ± 202.41
<i>GGM02S</i>	10.85 ± 11.39	2.55 ± 11.34	47.13 ± 201.64	10.81 ± 11.39	2.09 ± 11.35	57.78 ± 201.26
<i>TUM2S</i> ^b	7.84 ± 15.57	-4.05 ± 15.41	-5186.82 ± 1277.51	7.89 ± 15.56	-4.13 ± 15.40	-5380.69 ± 1249.48
<i>TUM1S</i> ^b	109.65 ± 15.79	48.90 ± 15.69	-4558.15 ± 1331.70	109.52 ± 15.80	49.10 ± 15.70	-4099.26 ± 1303.11
<i>EIGEN-GRACE02S</i>	-3.93 ± 6.66	-7.54 ± 6.58	-26.80 ± 99.00	-4.05 ± 6.66	-7.16 ± 6.59	-15.37 ± 98.63
<i>EIGEN-GRACE01S</i>	4.92 ± 27.56	-4.48 ± 27.60	-75.69 ± 218.43	4.52 ± 27.57	-5.74 ± 27.61	-69.51 ± 218.27
<i>EIGEN2</i>	10.82 ± 4.80	27.48 ± 4.78	1614.60 ± 236.93	10.75 ± 5.00	27.90 ± 4.96	1681.63 ± 244.16
<i>EIGEN1S</i>	15.92 ± 77.55	22.11 ± 85.44	1771.12 ± 2449.50	15.95 ± 77.53	22.26 ± 85.42	1766.71 ± 2444.99
<i>GRIM5C1</i>	35.36 ± 19.56	16.12 ± 19.94	453.23 ± 1139.51	35.18 ± 19.68	16.64 ± 20.07	616.06 ± 1131.74
<i>EGM96</i>	65.01 ± 5.24	15.86 ± 5.21	-1366.29 ± 2543.98	65.01 ± 5.24	15.86 ± 5.21	-1691.12 ± 2532.60

The differences of SHCs with their error variances up to $n_{\max} = 70$ have been used

^a The *first-degree* SHCs of the reference model *EIGEN-CG03C* and of the tested models *EIGEN-CG01C*, *EIGEN-CHAMP03S*, *TUM2S* and *TUM1S*, have been weighted according to the formal error estimates provided by the corresponding models. The (set-to-zero) *first-degree* SHCs of the models *EIGEN-GL04C*, *EIGEN-GRACE02S*, *EIGEN-GRACE01S*, *ITG-GRACE02S*, *GGM02C*, *GGM02S*, *EIGEN2*, *EIGEN1S*, *GRIM5C1* and *EGM96*, have been assumed errorless

^b The SHCs with their error variances up to $n_{\max} = 60$ have been used for testing these models

Table 7 Scale change of the inherent TRFs in various EGMs, which is obtained from the least-squares adjustment of Kleusberg’s transformation model (with respect to *EIGEN-CG03C*)

Model	Without taking into account zero- and first-degree SHC differences	Taking into account first-degree SHC differences ^a
	δs (ppb)	δs (ppb)
<i>EIGEN-GL04C</i>	91.55 ± 17.79	91.09 ± 17.81
<i>EIGEN-CG01C</i>	46.05 ± 23.17	45.60 ± 23.17
<i>EIGEN-CHAMP03S</i>	279.11 ± 103.80	280.19 ± 103.85
<i>ITG-GRACE02S</i>	28.21 ± 20.82	26.40 ± 21.01
<i>GGM02C</i>	194.95 ± 66.23	192.96 ± 66.26
<i>GGM02S</i>	391.72 ± 108.60	386.43 ± 108.59
<i>TUM2S</i> ^b	121.29 ± 59.31	121.13 ± 59.29
<i>TUM1S</i> ^b	−177.35 ± 55.82	−176.98 ± 55.84
<i>EIGEN-GRACE02S</i>	39.98 ± 38.97	41.01 ± 38.97
<i>EIGEN-GRACE01S</i>	101.09 ± 144.33	95.28 ± 144.33
<i>EIGEN2</i>	530.43 ± 24.83	533.03 ± 25.75
<i>EIGEN1S</i>	48.80 ± 125.57	48.94 ± 125.54
<i>GRIM5C1</i>	−43.74 ± 105.41	−44.25 ± 106.08
<i>EGM96</i>	46.77 ± 54.19	46.72 ± 54.20

The differences of SHCs with their error variances up to $n_{\max} = 70$ have been used

^a The *first-degree* SHCs of the reference model *EIGEN-CG03C* and of the tested models *EIGEN-CG01C*, *EIGEN-CHAMP03S*, *TUM2S* and *TUM1S*, have been weighted according to the formal error estimates provided by the corresponding models. The (set-to-zero) *first-degree* SHCs of the tested models *EIGEN-GL04C*, *EIGEN-GRACE02S*, *EIGEN-GRACE01S*, *ITG-GRACE02S*, *GGM02C*, *GGM02S*, *EIGEN2*, *EIGEN1S*, *GRIM5C1* and *EGM96*, have been assumed errorless

^b The SHCs with their error variances up to $n_{\max} = 60$ have been used for testing these models

Table 8 Example of the correlation matrix for the estimated TRF transformation parameters between *EIGEN-CG03C* and *EIGEN-CG01C*

	t_x	t_y	t_z	ε_x	ε_y	ε_z	δs
t_x	1.0000000	0.0010358	0.0001202	0.0003547	−0.0007009	−0.0010921	0.0154600
t_y		1.0000000	−0.0003548	0.0047606	−0.0007923	−0.0501770	−0.0025186
t_z			1.0000000	0.0011016	0.0100770	0.0062606	0.0072008
ε_x				1.0000000	−0.0012399	−0.0022621	−0.0001365
ε_y					1.0000000	0.0029371	0.0000217
ε_z						1.0000000	0.0001055
δs							1.0000000

highly inconsistent in terms of their zero-meridian reference planes, even within a 3σ confidence level (see the results for *EIGEN2*, *TUM1S* and *TUM2S*);

- the scale factor between the TRFs in the tested EGMs appears to be of the order $10^{-8} - 10^{-7}$, well above the ppb level. This mainly reflects the effect of various systematic errors and other inconsistencies that exist in the EGMs’ harmonic coefficients (for $n \geq 2$), which are ‘mapped’ to an apparent scale variation between their inherent TRFs. Note that, in Sect. 4.3, it is shown that most of these scale factors drop below the ppb level through the inclusion of

the difference $\bar{C}'_{0,0} - \bar{C}_{0,0}$ in the least-squares adjustment with Kleusberg’s model.

The square roots of the a posteriori variance factors for the previous adjustment tests are shown in Table 9. In most cases the values are close to 1, indicating that the diagonal weight matrix \mathbf{P} that was formed according to Eqs. (37) and (38) is quite realistic. The only exceptions occur for the tests with *TUM1S*, *TUM2S* and *GRIM5C1*, which reveal that the original error variances for their SHCs are rather optimistic.

Table 9 Square root of the a posteriori variance factor for the least-squares adjustments corresponding to the various cases shown in Tables 5, 6 and 7

Model	Without taking into account zero- and first-degree SHC differences	Taking into account first-degree SHC differences
<i>EIGEN-GL04C</i>	0.77	0.77
<i>EIGEN-CG01C</i>	0.78	0.78
<i>EIGEN-CHAMP03S</i>	1.60	1.60
<i>ITG-GRACE02S</i>	1.26	1.28
<i>GGM02C</i>	1.50	1.51
<i>GGM02S</i>	1.49	1.49
<i>TUM2S</i>	3.02	3.02
<i>TUM1S</i>	2.63	2.64
<i>EIGEN-GRACE02S</i>	1.01	1.01
<i>EIGEN-GRACE01S</i>	0.73	0.73
<i>EIGEN2</i>	1.19	1.23
<i>EIGEN1S</i>	1.87	1.87
<i>GRIM5C1</i>	6.44	6.49
<i>EGM96</i>	1.85	1.85

Note that all accuracy estimates given in Tables 5, 6 and 7 have been re-scaled in order to account for the a posteriori variance factor that was obtained in each case.

4.2 Using $\{\bar{C}_{nm}, \bar{S}_{nm}\}$ and $\{\bar{C}'_{nm}, \bar{S}'_{nm}\}$ for $n \geq 1$

Another series of adjustment tests was performed by including the differences $\bar{C}'_{1,0} - \bar{C}_{1,0}$, $\bar{C}'_{1,1} - \bar{C}_{1,1}$ and $\bar{S}'_{1,1} - \bar{S}_{1,1}$ in the observation vector \mathbf{y} . In all cases, the first-degree SHCs $\bar{C}_{1,0}$, $\bar{C}_{1,1}$, $\bar{S}_{1,1}$ were equal to the formal non-zero values provided by the *EIGEN-CG03C* model, whereas $\bar{C}'_{1,0}$, $\bar{C}'_{1,1}$, $\bar{S}'_{1,1}$ were either conventionally equal to zero (*EIGEN-GL04C*, *ITG-GRACE02S*, *GGM02C*, *GGM02S*, *EIGEN-GRACE02S*, *EIGEN-GRACE01S*, *EIGEN2*, *EIGEN1S*, *GRIM5C1*, *EGM96*), or equal to their formal non-zero values (*EIGEN-CG01C*, *EIGEN-CHAMP03S*, *TUM2S*, *TUM1S*).

The statistical weights for the three additional ‘observations’ have been determined according to Eqs. (37) and (38) by taking into account the error variances for the corresponding first-degree SHCs. In the case of *EIGEN-GL04C*, *ITG-GRACE02S*, *GGM02C*, *GGM02S*, *EIGEN-GRACE02S*, *EIGEN-GRACE01S*, *EIGEN2*, *EIGEN1S*, *GRIM5C1* and *EGM96* (where $\bar{C}'_{1,0}$, $\bar{C}'_{1,1}$, $\bar{S}'_{1,1}$ are a priori fixed to zero), it has been assumed that $\sigma_{\bar{C}'_{1,0}} = \sigma_{\bar{C}'_{1,1}} = \sigma_{\bar{S}'_{1,1}} = 0$.

The adjustment results are shown in the corresponding columns of Tables 5, 6, 7 and 9. The only notable difference with respect to the results of the previous section are the significantly smaller values for the translation parameters and the improvement of their accuracy level. The origins of the EGMs’ reference frames appear now to be consistent

at the *cm*-level, with their total shift ranging from a few mm up to approximately 2.5 cm. This indicates that the inclusion of the first-degree SHC differences in the least-squares adjustment with Kleusberg’s model acts as an effective ‘filter’ for various systematic errors in the EGMs’ coefficients (for $n \geq 2$), which corrupted significantly the estimated translation parameters in the previous adjustment scenario (Sect. 4.1).

The TRF orientation and scale parameters do not show significant variations in their estimated values when the first-degree SHCs are taken into account, and they appear to follow the same pattern that was indicated in Sect. 4.1. The actual changes in the rotation angle ε_z are more pronounced than the changes in the other two rotation parameters, yet they remain within their 1σ uncertainty level.

In order to obtain a more realistic assessment of the origin consistency between the EGMs’ reference frames, an additional series of adjustment tests was performed for the models *EIGEN-GL04C*, *ITG-GRACE02S*, *GGM02C*, *GGM02S*, *EIGEN-GRACE02S*, *EIGEN-GRACE01S*, *EIGEN2*, *EIGEN1S*, *GRIM5C1* and *EGM96*. Note that the previous results for these particular models were based on a zero-uncertainty assumption for their first-degree harmonics, and thus the weights of the differences $\bar{C}'_{1,0} - \bar{C}_{1,0}$, $\bar{C}'_{1,1} - \bar{C}_{1,1}$, $\bar{S}'_{1,1} - \bar{S}_{1,1}$ were calculated based solely on the (formal) first-degree SHC error variances of the reference model *EIGEN-CG03C*.

For the new tests, the (set-to-zero) first-degree SHCs of the aforementioned ten models have been assigned a standard uncertainty level of $\sim 4.526 \times 10^{-10}$, which corresponds to a uniform *EGM-geocentricity accuracy* of $\sigma_{x_{cm}} = \sigma_{y_{cm}} = \sigma_{z_{cm}} = \pm 5\text{mm}$; see Eqs. (13)–(15). The results for the TRF transformation parameters in this case are collectively given in Table 10.

From the results in Table 10, it is seen that the estimated translation parameters remain within the same order of magnitude as in Table 5. Basically, only the t_z values are changed by a few mm for some EGMs (notable exception is the case of *GRIM5C1* where all three translation parameters change their values by 4, 2 and 9 mm, respectively). The changes in the TRF rotation and scale parameters are negligible with respect to the corresponding values shown in Tables 6 and 7.

4.3 Using $\{\bar{C}_{nm}, \bar{S}_{nm}\}$ and $\{\bar{C}'_{nm}, \bar{S}'_{nm}\}$ for $n \geq 0$

The difference of the zero-degree SHCs was excluded from the input data \mathbf{y} in all previous adjustment tests. Even if this difference is a priori equal to zero (which is the case for EGMs using the same conventional values for GM), the inclusion of $\bar{C}'_{0,0} - \bar{C}_{0,0}$ in the least-squares adjustment of Kleusberg’s model leads to a more realistic estimation of the scale factor

Table 10 Similarity transformation parameters of the inherent TRFs in various EGMs obtained from the least-squares adjustment of Kleusberg’s transformation model (with respect to *EIGEN-CG03C*)

Model	t_x (mm)	t_y (mm)	t_z (mm)	ε_x (mas)	ε_y (mas)	ε_z (mas)	δs (ppb)
<i>EIGEN-GL04C</i>	5.9 ± 5.4	0.1 ± 5.4	16.9 ± 5.1	5.04 ± 3.75	-0.88 ± 3.73	-71.04 ± 53.35	91.09 ± 17.80
<i>EIGEN-GRACE02S</i>	6.0 ± 7.0	1.3 ± 7.3	12.3 ± 6.6	-4.05 ± 6.66	-7.16 ± 6.59	-15.38 ± 98.63	40.99 ± 38.97
<i>EIGEN-GRACE01S</i>	5.5 ± 5.1	0.5 ± 5.4	15.6 ± 4.9	4.52 ± 27.57	-5.74 ± 27.61	-69.51 ± 218.27	95.28 ± 144.33
<i>ITG-GRACE02S</i>	6.3 ± 8.8	0.0 ± 8.8	32.1 ± 8.3	-4.02 ± 4.45	-6.96 ± 4.44	-85.90 ± 64.79	26.41 ± 21.00
<i>GGM02C</i>	5.3 ± 10.5	0.9 ± 10.4	18.3 ± 9.9	17.82 ± 11.51	10.72 ± 11.12	102.92 ± 202.41	192.98 ± 66.26
<i>GGM02S</i>	5.3 ± 10.4	0.9 ± 10.4	18.1 ± 9.8	10.81 ± 11.39	2.09 ± 11.35	57.77 ± 201.26	386.47 ± 108.59
<i>EIGEN2</i>	3.6 ± 8.6	1.3 ± 8.5	6.2 ± 8.2	10.75 ± 4.97	27.90 ± 4.95	1681.49 ± 244.15	533.03 ± 25.75
<i>EIGEN1S</i>	5.5 ± 13.0	0.3 ± 13.0	15.2 ± 12.4	15.95 ± 77.53	22.26 ± 85.42	1766.71 ± 2444.99	48.94 ± 125.54
<i>GRIM5C1</i>	13.5 ± 45.0	4.4 ± 44.9	-1.1 ± 43.0	35.18 ± 19.68	16.64 ± 20.07	615.31 ± 1131.81	-44.24 ± 106.08
<i>EGM96</i>	5.7 ± 12.9	0.2 ± 12.8	15.0 ± 12.2	65.01 ± 5.24	15.86 ± 5.21	-1691.11 ± 2532.59	46.72 ± 54.20

The differences of SHCs with their error variances up to $n_{\max} = 70$ have been used, including the first-degree harmonics from all models. The *first-degree* SHCs of the reference model *EIGEN-CG03C* have been weighted according to their formal error estimates. The (set-to-zero) *first-degree* SHCs of all tested models have been weighted by adopting a uniform ‘geocentricity’ accuracy of ± 5 mm

δs between the EGMs’ reference frames, as we shall see from the following results.

A crucial aspect in this case is the proper weighting of the zero-degree SHCs, which should be based on the uncertainty of the geocentric gravitational ‘constant’ that is adopted by each geopotential model. Even if the underlying EGMs use the same conventional GM, the realized scale of their associated TRFs is affected by the physical ambiguity of its value (Zhu et al. 2001) which is mostly concentrated on the zero-degree harmonic term.

For the tests presented in this section, the difference $\bar{C}'_{0,0} - \bar{C}_{0,0}$ is included as additional observation in the least-squares adjustment of Kleusberg’s model, with its weight set to

$$p = \frac{1}{\sigma_{\bar{C}'_{0,0}}^2 + \sigma_{\bar{C}_{0,0}}^2} \tag{39}$$

The error variances for the zero-degree SHCs are determined from Eq. (6) using the IERS standard uncertainty of $\sigma_{GM} = 0.8 \times 10^6 \text{ m}^3 \text{ s}^{-2}$ (McCarthy and Petit 2004). In some of the tested models their zero-degree coefficient is already accompanied by a formal error estimate (see Table 2). For these cases, the value of $\sigma_{\bar{C}'_{0,0}}$ in Eq. (39) corresponds to the one provided by the corresponding EGM solution, and not to the value implied by the IERS uncertainty for GM.

The treatment of the first-degree SHCs is similar to the approach followed in the previous section. In particular, the differences $\bar{C}'_{1,0} - \bar{C}_{1,0}$, $\bar{C}'_{1,1} - \bar{C}_{1,1}$, $\bar{S}'_{1,1} - \bar{S}_{1,1}$ are included in the adjustment and they have been weighted according to the formal error variances of the first-degree SHCs of the corresponding models. In cases where the first-degree coefficients of the tested model are conventionally set to zero, their error variances have been computed by adopting a uniform EGM-geocentricity accuracy level of ± 5 mm.

The results for the estimated TRF transformation parameters and their accuracy level are given in Table 11, whereas the square roots of the a posteriori variance factor for each adjustment are shown in Table 12. *These results should be considered as our most representative assessment for the TRF consistency among the 15 tested EGMs.*

Based on the values in Table 11, the following comments can be made

- the TRFs associated with most of the tested EGMs show a scale stability at the ppb level, or better. Notable exceptions are the models *TUMIS* and *EIGEN2*, where the estimated scale factor reaches the values of -15.57 and 9.64 ppb, respectively;
- the translation and rotation parameters are essentially unaffected by the inclusion of the difference $\bar{C}'_{0,0} - \bar{C}_{0,0}$ in the least-squares adjustment, and they practically retain the same estimated values (and accuracy level) that were obtained in the previous adjustment tests in Sect. 4.2.

In order to assess the effect of the estimated differences among the EGMs’ reference frames on the height anomaly signal computed from their SHCs, we shall consider the datum transformation formula

$$\zeta' - \zeta = \delta\zeta(t_x, t_y, t_z) + \delta\zeta(\varepsilon_x, \varepsilon_y) + \delta\zeta(\delta s) \tag{40}$$

where the individual transformation terms are analytically given by the equations (e.g. Rapp 1993; Kotsakis 2008)

$$\delta\zeta(t_x, t_y, t_z) = t_x \cos\varphi \cos\lambda + t_y \cos\varphi \sin\lambda + t_z \sin\varphi \tag{41}$$

$$\delta\zeta(\varepsilon_x, \varepsilon_y) = \frac{ae^2}{W} (-\varepsilon_x \sin\varphi \cos\varphi \sin\lambda + \varepsilon_y \sin\varphi \cos\varphi \cos\lambda) \tag{42}$$

$$\delta\zeta(\delta s) = (aW + \zeta)\delta s \tag{43}$$

Table 11 Similarity transformation parameters of the inherent TRFs in various EGMs obtained from the least-squares adjustment of Kleusberg's transformation model (with respect to *EIGEN-CG03C*)

Model	t_x (mm)	t_y (mm)	t_z (mm)	ε_x (mas)	ε_y (mas)	ε_z (mas)	δs (ppb)
<i>EIGEN-GL04C</i>	5.8 ± 5.4	0.1 ± 5.4	16.9 ± 5.1	5.04 ± 3.76	-0.88 ± 3.74	-71.04 ± 53.48	1.36 ± 2.18
<i>EIGEN-CG01C</i>	2.1 ± 6.0	2.2 ± 6.0	4.2 ± 5.5	-0.67 ± 4.11	-2.82 ± 4.09	95.21 ± 61.40	0.42 ± 2.21
<i>EIGEN-CHAMP03S</i>	2.7 ± 9.4	1.0 ± 9.3	5.6 ± 8.8	15.98 ± 22.18	20.52 ± 22.02	-582.88 ± 356.97	0.53 ± 4.53
<i>ITG-GRACE02S</i>	6.3 ± 8.8	0.0 ± 8.8	32.1 ± 8.3	-4.02 ± 4.45	-6.96 ± 4.44	-85.90 ± 64.80	0.76 ± 3.57
<i>GGM02C</i>	5.2 ± 10.5	0.9 ± 10.5	18.3 ± 9.9	17.83 ± 11.51	10.72 ± 11.13	102.92 ± 202.56	0.80 ± 4.27
<i>GGM02S</i>	5.3 ± 10.4	0.9 ± 10.4	18.1 ± 9.9	10.82 ± 11.41	2.11 ± 11.36	57.75 ± 201.49	0.59 ± 4.24
<i>TUM2S</i> ^a	5.7 ± 14.6	0.7 ± 14.6	15.8 ± 13.2	7.89 ± 15.57	-4.13 ± 15.41	-5380.53 ± 1249.97	2.29 ± 6.02
<i>TUM1S</i> ^a	4.3 ± 12.8	-1.1 ± 12.8	-0.6 ± 11.5	109.52 ± 15.81	49.10 ± 15.71	-4099.30 ± 1304.46	-15.57 ± 5.27
<i>EIGEN-GRACE02S</i>	5.9 ± 7.0	1.3 ± 7.3	12.3 ± 6.6	-4.05 ± 6.66	-7.16 ± 6.59	-15.38 ± 98.63	0.22 ± 2.85
<i>EIGEN-GRACE01S</i>	5.5 ± 5.1	0.5 ± 5.4	15.6 ± 4.9	4.53 ± 27.57	-5.74 ± 27.61	-69.52 ± 218.25	0.02 ± 2.08
<i>EIGEN2</i>	3.4 ± 8.9	1.3 ± 8.9	6.1 ± 8.5	10.75 ± 5.18	27.90 ± 5.16	1681.90 ± 254.12	9.64 ± 3.60
<i>EIGEN1S</i>	5.5 ± 13.0	0.3 ± 13.0	15.2 ± 12.4	15.95 ± 77.52	22.26 ± 85.41	1766.71 ± 2444.75	0.09 ± 5.31
<i>GRIM5C1</i>	13.5 ± 45.0	4.4 ± 44.9	-1.1 ± 43.0	35.18 ± 19.68	16.64 ± 20.07	615.28 ± 1131.68	-0.77 ± 12.92
<i>EGM96</i>	5.7 ± 12.9	0.2 ± 12.8	15.0 ± 12.2	65.01 ± 5.24	15.86 ± 5.21	-1691.20 ± 2532.53	0.43 ± 5.22

The differences of SHCs with their error variances up to $n_{\max} = 70$ have been used, including the zero- and first-degree harmonics from all models. The *first-degree* SHCs of the reference model *EIGEN-CG03C* and of the tested models *EIGEN-CG01C*, *EIGEN-CHAMP03S*, *TUM2S* and *TUM1S*, have been weighted according to the formal error estimates provided by the corresponding models. The (set-to-zero) *first-degree* SHCs of the tested models *EIGEN-GL04C*, *EIGEN-GRACE02S*, *EIGEN-GRACE01S*, *ITG-GRACE02S*, *GGM02C*, *GGM02S*, *EIGEN2*, *EIGEN1S*, *GRIM5C1* and *EGM96*, have been weighted by adopting a uniform 'geocentricity' accuracy of ±5 mm. The *zero-degree* SHC of the tested models *TUM2S*, *TUM1S* and *GRIM5C1* has been weighted according to the formal error estimate $\sigma_{\zeta_{00}}$ provided by the corresponding models. The (set-to-one) *zero-degree* SHC of the reference model *EIGEN-CG03C* and of the tested models *EIGEN-GL04C*, *EIGEN-CG01C*, *EIGEN-CHAMP03S*, *EIGEN-GRACE02S*, *EIGEN-GRACE01S*, *ITG-GRACE02S*, *GGM02C*, *GGM02S*, *EIGEN2*, *EIGEN1S* and *EGM96*, has been weighted by adopting the IERS standard uncertainty level of the geocentric gravitational constant $\sigma_{GM} = 0.8 \times 10^6 \text{ m}^3 \text{ s}^{-2}$

^a The SHCs with their error variances up to $n_{\max} = 60$ have been used for testing these models

Table 12 Square root of the a posteriori variance factor for the least-squares adjustments corresponding to the various cases shown in Table 11

Model	$\hat{\sigma}_o$
<i>EIGEN-GL04C</i>	0.77
<i>EIGEN-CG01C</i>	0.78
<i>EIGEN-CHAMP03S</i>	1.60
<i>ITG-GRACE02S</i>	1.28
<i>GGM02C</i>	1.51
<i>GGM02S</i>	1.49
<i>TUM2S</i>	3.02
<i>TUM1S</i>	2.64
<i>EIGEN-GRACE02S</i>	1.01
<i>EIGEN-GRACE01S</i>	0.73
<i>EIGEN2</i>	1.28
<i>EIGEN1S</i>	1.87
<i>GRIM5C1</i>	6.49
<i>EGM96</i>	1.85

Due to the rotational symmetry of the reference ellipsoid involved in the calculation of ζ , the rotation angle ε_z does not affect the transformation of the height anomaly between different TRFs. The auxiliary quantity W corresponds to the unitless expression

$$W = (1 - e^2 \sin^2 \varphi)^{1/2} \quad (44)$$

while the length of the semi-major axis a and the squared eccentricity e^2 that appear in the previous equations define the geometry of the adopted reference ellipsoid for the height anomaly determination.

Using the transformation parameters from Table 11, the statistics of the height anomaly differences due to TRF translation $\delta\zeta(t_x, t_y, t_z)$, TRF rotation $\delta\zeta(\varepsilon_x, \varepsilon_y)$, and TRF scale variation $\delta\zeta(\delta s)$ have been computed over a test area enclosing most of the Canadian territory ($48^\circ \text{ N} < \varphi < 68^\circ \text{ N}$, $240^\circ \text{ W} < \lambda < 290^\circ \text{ W}$). Our numerical calculations have been performed on a $1^\circ \times 1^\circ$ grid within the above geographical limits, using *EIGEN-CG03C* as the reference model associated with the initial ζ values with respect to the GRS80 ellipsoid. The statistics for the individual transformation components, as well as for the total height anomaly variation, are given in Table 13.

Although the orientation differences among the EGMs' reference frames have a negligible effect ($< 1 \text{ cm}$) on the height anomaly signal, the combined effect of their TRF origin and scale differences can reach several cm, as it can be seen from Table 13. In all cases, the total TRF effect appears as an almost constant bias in the height anomaly signal, since

Table 13 Statistics (in cm) of height anomaly variations induced by the EGM/TRF transformation parameters shown in Table 11

Model	$\delta\zeta(t_x, t_y, t_z)$		$\delta\zeta(\varepsilon_x, \varepsilon_y)$		$\delta\zeta(\delta s)$		$\delta\zeta_{\text{total}}$	
	μ	σ	μ	σ	μ	σ	μ	σ
<i>EIGEN-GL04C</i>	1.4	0.1	0.0	0.0	0.9	0.0	2.3	0.1
<i>EIGEN-CG01C</i>	0.2	0.1	0.0	0.0	0.3	0.0	0.5	0.0
<i>EIGEN-CHAMP03S</i>	0.4	0.1	0.1	0.1	0.3	0.0	0.9	0.1
<i>ITG-GRACE02S</i>	2.7	0.2	0.0	0.0	0.5	0.0	3.1	0.2
<i>GGM02C</i>	1.5	0.1	0.1	0.0	0.5	0.0	2.1	0.1
<i>GGM02S</i>	1.5	0.1	0.1	0.0	0.4	0.0	1.9	0.1
<i>TUM2S</i>	1.3	0.1	0.1	0.0	1.5	0.0	2.8	0.1
<i>TUM1S</i>	0.0	0.1	0.9	0.2	-9.9	0.0	-9.0	0.2
<i>EIGEN-GRACE02S</i>	0.9	0.1	0.0	0.0	0.1	0.0	1.1	0.1
<i>EIGEN-GRACE01S</i>	1.3	0.1	0.0	0.0	0.0	0.0	1.3	0.1
<i>EIGEN2</i>	0.4	0.1	0.1	0.1	6.1	0.0	6.6	0.1
<i>EIGEN1S</i>	1.2	0.1	0.1	0.1	0.1	0.0	1.4	0.2
<i>GRIM5C1</i>	-0.4	0.2	0.3	0.1	-0.5	0.0	-0.6	0.2
<i>EGM96</i>	1.2	0.1	0.6	0.1	0.3	0.0	2.1	0.1

The calculations refer to a uniform $1^\circ \times 1^\circ$ geographical grid, over a test area that encloses most of the Canadian territory ($48^\circ\text{N} < \varphi < 68^\circ\text{N}$, $240^\circ\text{W} < \lambda < 290^\circ\text{W}$). All values refer to the differences with respect to the height anomaly signal obtained by *EIGEN-CG03C* using the GRS80 reference ellipsoid

the dispersion (σ) of its values over the test area is always well below the *cm*-level.

4.4 The sensitivity of the estimated TRF transformation parameters with respect to the maximum harmonic degree of the SHC differences $\{\bar{C}'_{nm} - \bar{C}_{nm}\}$ and $\{\bar{S}'_{nm} - \bar{S}_{nm}\}$

It is well known that the sensitivity of the geopotential SHCs with respect to their underlying TRF is confined to the very low-degree spectral band (Kleusberg 1980; Pavlis 1998). An additional series of tests has been performed to explore the reverse aspect of the previous statement, namely the sensitivity of the estimated TRF transformation parameters (obtained through Kleusberg’s model) with respect to the spectral bandwidth of the used SHCs. The results shown in the following graphs have been obtained by using Kleusberg’s formulae for the joint adjustment of $\{\bar{C}'_{nm} - \bar{C}_{nm}\}$ and $\{\bar{S}'_{nm} - \bar{S}_{nm}\}$, and setting successively increasing values for the maximum harmonic degree of the ingoing SHC differences.

As in the previous tests, *EIGEN-CG03C* is adopted as the reference model with respect to which the TRF transformation parameters of the other EGMs are determined. Here, we present results for the max/degree-dependent variations in the estimated transformation parameters for *EIGEN-GRACE02S*, *GGM02C* and *EIGEN-CHAMP03S*; see Figs. 3, 4, 5. The successive least-squares adjustments with Kleusberg’s model have been based on the same general scenario that was followed in Sect. 4.3 (i.e. inclusion of both zero- and first-degree SHC differences with appropriate statistical weights for each case).

From Fig. 3 we see that the TRF translation parameters remain practically constant after $n_{\text{max}} \approx 10$, thus indicating that the very low-degree coefficients are the ones that essentially contribute to the estimation of t_x, t_y, t_z through the inversion of Kleusberg’s model. It is interesting to point out that, in the case of *EIGEN-CHAMP03S*, the estimated translation parameters change much less (as n_{max} increases) compared to the other two geopotential models. The reason for that is that both *EIGEN-CG03C* and *EIGEN-CHAMP03S* are already accompanied by some a priori information for their TRF origin offset with respect to the geocenter (i.e. the first-degree SHCs of both models are not fixed to zero), and thus the results of the least-squares adjustment likely tend to converge to much closer values for the TRF translation parameters, as n_{max} increases.

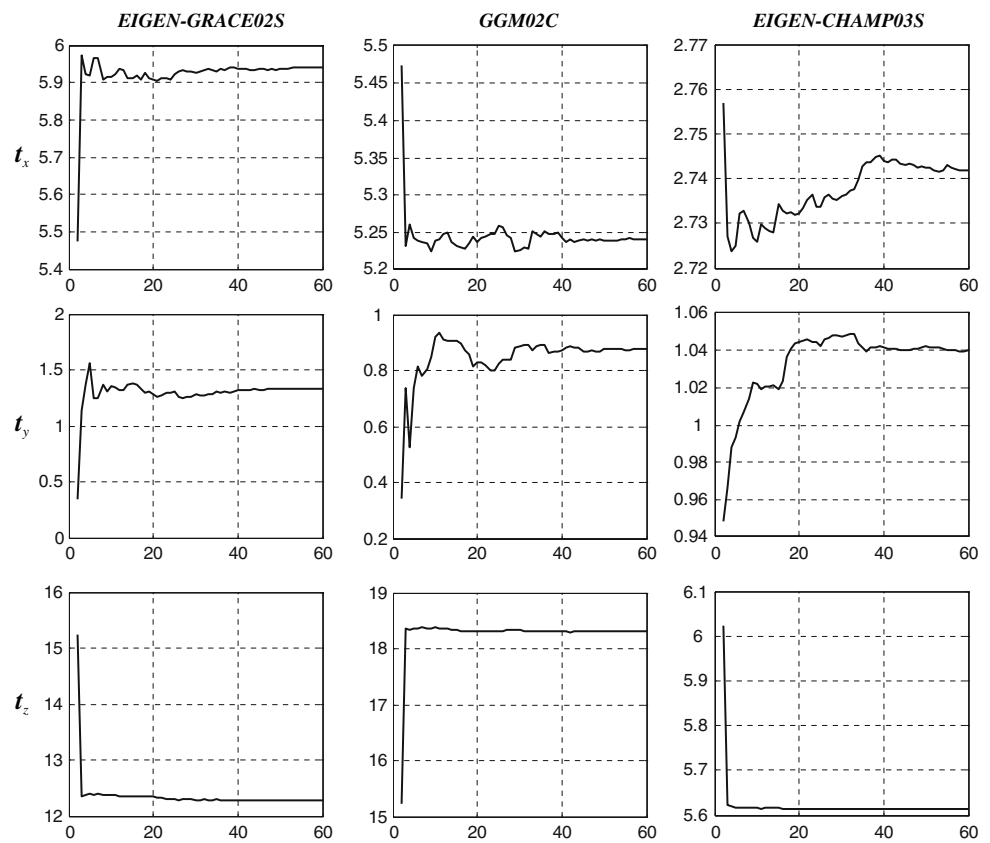
The variations for the EGMs’ reference frame rotations are shown in Fig. 4. Notice that the estimated rotation angles ε_x and ε_y exhibit very small variability (less than 1–2 mas) as n_{max} increases, and they remain practically constant for $n_{\text{max}} > 40$. The third rotation angle ε_z shows higher variability with considerably larger values for its absolute magnitude, yet it also remains constant for $n_{\text{max}} > 40$.

Finally, the behavior of the estimated scale factor as a function of n_{max} is shown in Fig. 5, where we see that the δs -variations are negligible (less than 0.1 ppb) over the entire spectral band that was considered for these tests.

5 Conclusions

Using Kleusberg’s (1980) formulation for the TRF transformation of Earth’s gravitational potential SHCs, a number of

Fig. 3 Estimated TRF translation parameters (in mm) between *EIGEN-CG03C* and three tested geopotential models (*EIGEN-GRACE02S*, *GGM02C*, *EIGEN-CHAMP03S*) as a function of the maximum harmonic degree used in the least-squares adjustment with Kleusberg's model



geopotential models have been tested in terms of their TRF consistency with respect to the reference frame underlying the *EIGEN-CG03C* model. Compared to other techniques that have been used for similar purposes (e.g. comparisons between geometric and gravimetric geoid undulations over control networks of GPS/leveling benchmarks), our methodology solely relies on the adjustment of SHC differences, $\{\bar{C}'_{nm} - \bar{C}_{nm}\}$ and $\{\bar{S}'_{nm} - \bar{S}_{nm}\}$, according to a similarity (linearized Helmert-type) transformation model that relates the TRFs in the corresponding EGMs.

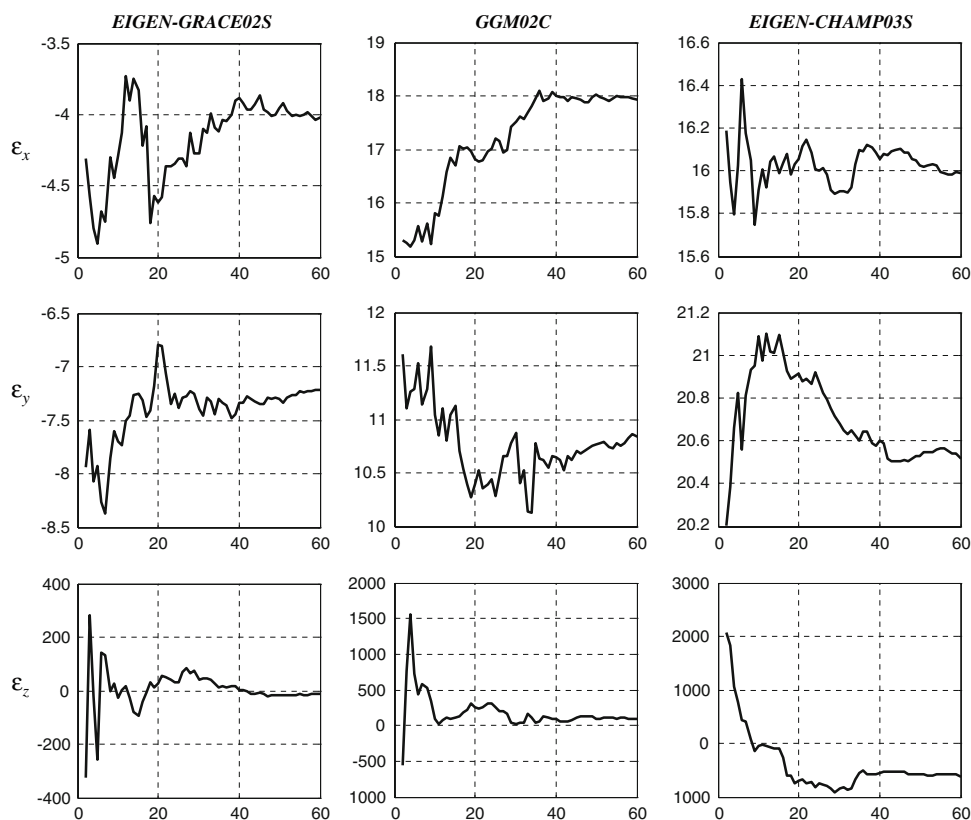
Based on the findings of our study, the following conclusions can be stated:

- the TRFs of the tested EGMs show a consistency for their origin position at the level of 1–2 cm or better. Notable exception are the results obtained for *ITG-GRACE02S*, which revealed a spatial origin shift ($\sqrt{t_x^2 + t_y^2 + t_z^2}$) of 3.3 cm with respect to *EIGEN-CG03C*, mainly due to a large offset in the t_z component. Note, however, that in most cases the uncertainty of the estimated translation parameters is considerably larger than the actual magnitude of their values (with the exception of t_z in several EGMs — see Table 11), a fact that indicates the inherent difficulty of extracting TRF

information from geopotential models at the currently available accuracy level of their SHCs (more comments to follow on this issue);

- a result that requires further study is the evident bias in the t_z values, compared to the equatorial translation components t_x and t_y . In most of the tested EGMs, the TRF translation parameter t_z shows systematically larger values than the other two translation components. Note that a similar *z-shift effect* has been repeatedly reported by several authors in the context of global TRF studies (e.g. [Schaab and Groten 1979](#); [Grappo 1980](#); [West 1982](#); [Soler and van Gelder 1987](#); [Boucher and Altamimi 2001](#); [Heflin et al. 2002](#));
- in terms of orientation stability for the mean Earth rotation axis (rotation angles ε_x and ε_y), the associated TRFs of the tested EGMs show variations in the order of 10^{-2} – 10^{-3} arcsec. The rotation angle ε_z appears to have larger values by 1–3 orders of magnitude (up to a few arcsec), a fact that does not necessarily suggest the existence of systematic differences in the realization of the zero-meridian plane among the EGMs' reference frames, since the corresponding uncertainty of ε_z is, in most cases, quite high (see Table 11). It should be kept in mind that there is a natural deficiency involved in the precise

Fig. 4 Estimated TRF rotation angles (in mas) between *EIGEN-CG03C* and three tested geopotential models (*EIGEN-GRACE02S*, *GGM02C*, *EIGEN-CHAMP03S*) as a function of the maximum harmonic degree used in the least-squares adjustment with Kleusberg's model



estimation of ε_z exclusively from SHCs, due to the (almost) rotationally-symmetric behavior of Earth's gravitational field;

- the TRF scale stability in most of the tested EGMs is at the sub-ppb level, although for some models (*EIGEN2*, *TUMIS*) scale factors δs well above the ppb-level have been estimated. It should be also noted that the effect of various systematic errors in the EGMs' harmonic coefficients (for $n \geq 2$) can cause an apparent scale variation in their inherent TRFs at the level of $10^{-8} - 10^{-7}$ (see Tables 7 and 10).

A few remarks about the feasibility of Kleusberg's model as a testing tool for the TRF consistency in different EGMs should finally be stated. Undoubtedly, the estimated transformation parameters that we obtain through the least-squares inversion of Kleusberg's model do not only reflect the possible differences in the TRFs underlying each EGM solution, but they also contain effects from other 'error signals' that exist in the original SHCs. Although the random part of these errors is effectively filtered, within the adjustment procedure, through the data weight matrix \mathbf{P} (see Sect. 3), there still remains the risk that certain systematic-type signals will be lumped into the estimated transformation parameters and thus cause apparent differences in the EGM-related TRFs.

Note that the EGMs tested in this paper are mainly 'static' models and they were developed from various data sets with quite different time spanning periods, some as short as a few months while other covering decades. Furthermore, the determination of their SHCs imply that certain temporal aspects of Earth's gravitational field (e.g. tidal variations, loading effects, mass re-distribution within Earth's system) are modeled in a specific fashion, which is not necessarily identical for each geopotential solution. The temporal variations of Earth's gravitational field are inevitably averaged over the time span of each data set, and then aliased onto the estimated SHCs of each model. As a result, the transformation parameters obtained from the inversion of Kleusberg's formulae will be partially affected by the inconsistencies that may exist in the treatment of various temporal effects within each 'static' EGM solution.

Nevertheless, it should be noted that the situation described above is not much different from what is practically involved in several other TRF studies. Take, for example, the estimation of the similarity transformation parameters between a global geodetic datum (e.g. ITRF_{xx}) and a local geodetic datum, based on the 3D Cartesian coordinates for a group of terrestrial control points. In our case, instead of common points we have a common signal (i.e. the gravitational potential function $V(\cdot)$) and the role of coordi-

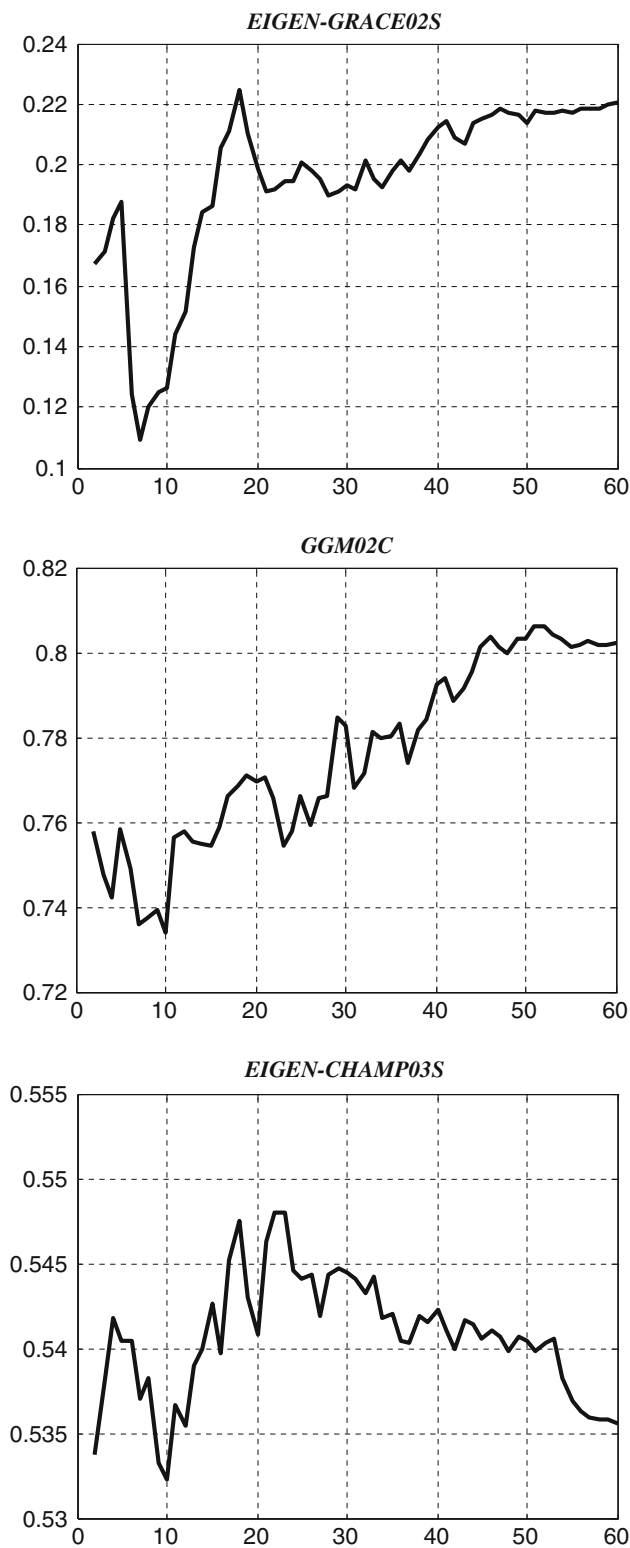


Fig. 5 Estimated TRF scale factor (in ppb) between *EIGEN-CG03C* and three tested geopotential models (*EIGEN-GRACE02S*, *GGM02C*, *EIGEN-CHAMP03S*) as a function of the maximum harmonic degree used in the least-squares adjustment with Kleusberg's model

nates is undertaken by the known SHCs of $V(\cdot)$ with respect to different geopotential models, each of which carries its own realization of an Earth-fixed reference system. In many TRF studies, the known coordinates in the local datum often refer to a different epoch than the available spatial positions in the global datum, without being associated with a regional velocity model for their temporal variations. Furthermore, their values are usually affected by various unknown systematic errors due to the improper (sub-optimal) processing of heterogeneous geodetic measurements, some of which may cover an extended time period while others may refer to more recent observation campaigns. Similar problems also arise in EGM evaluation and TRF-testing studies using GPS/levelling heights, where the final results are often obscured by several systematic error sources existing in the original height data.

Let us finally underline that the SHCs of Earth's gravitational field are certainly not the most accurate sensors of TRF information, a fact which has been reflected in our results via the comparatively large standard deviations for the estimated transformation parameters. Compared to the 3D Cartesian coordinates with respect to a global TRF (which can be known with an accuracy of a few mm at a given epoch), the relative uncertainty of the geopotential SHCs is actually worse by 1–4 orders of magnitude. This shortcoming, however, is partially compensated by the advantage of Kleusberg's model to inflict a *uniform and global* spatial coverage of TRF information, as it does not rely on the Cartesian coordinates of irregularly distributed control points over a sparse terrestrial network, but it uses the spectral coordinates (i.e. SHCs) of a continuous signal that is realized over the entire Earth's surface.

Acknowledgments The author would like to acknowledge the valuable suggestions and comments that were provided by E.C. Pavlis, C. Förste and an anonymous reviewer.

References

- Anderle RJ (1974) Transformation of terrestrial survey data to Doppler satellite datum. *J Geophys Res* 79(B35):5319–5331
- Balmino G, Borderies N (1978) Gravitational potential of solid bodies in the solar system. *Celest Mech* 17(2):113–119
- Boucher C, Altamimi Z (2001) ITRS, PZ-90 and WGS84: current realizations and the related transformation parameters. *J Geod* 75(11):613–619
- Cook GE (1963) Perturbations of satellite orbits by tesseral harmonics in the Earth's gravitational potential. *Plan Space Sci* 11:797–815
- Ditmar P, Kuznetsov V, van Eck van der Sluijs AA, Schrama E, Klees R (2006) 'DEOS_CHAMP-01C_70': a model of the Earth's gravity field computed from accelerations of the CHAMP satellite. *J Geod* 79(10/11):586–601
- Eckhardt DH (1984) Correlations between global features of terrestrial fields. *Math Geol* 16(2):155–171

- Ekman M (1989) Impacts of geodynamic phenomena on systems for height and gravity. *Bull Geod* 63(3):281–296
- Engelis T (1985) Global circulation from SEASAT altimeter data. *Mar Geod* 9:45–69
- Földvary L, Svehla D, Gerlach C, Wermuth M, Gruber T, Rummel R, Rothacher M, Frommknecht B, Peters T, Steigenberger P (2005) Gravity model TUM-2Sp based on the energy balance approach and kinematic CHAMP orbits. In: Reigber C, Luhr H, Schwintzer P, Wickert J (eds) *Earth observation with CHAMP—results from three years in orbit*. Springer, Berlin, pp 13–18
- Förste C, Flechtner F, Schmidt R, Meyer U, Stubenvoll R, Barthelmes F, Rothacher M, Biancale R, Bruinsma S, Lemoine J-M (2005) A new high resolution global gravity field model from the combination of GRACE satellite mission and altimetry/gravimetry surface gravity data. Poster presented at the EGU General Assembly, Vienna, Austria, April 24–29, 2005, *Geophysical Research Abstracts*, vol. 7:04561
- Förste C, Flechtner F, Schmidt R, König R, Meyer U, Stubenvoll R, Rothacher M, Barthelmes F, Neumayer KH, Biancale R, Bruinsma S, Lemoine J-M (2006) A mean global gravity field model from the combination of satellite mission and altimetry/gravimetry surface gravity data. Poster presented at the EGU General Assembly, Vienna, Austria, April 2–7, 2006, *Geophysical Research Abstracts*, vol 8:03462
- Gerlach C, Földvary L, Svehla D, Gruber T, Wermuth M, Sneeuw N, Frommknecht B, Oberndorfer H, Peters T, Rothacher M, Rummel R, Steigenberger P (2003) A CHAMP-only gravity field model from kinematic orbits using the energy integral. *Geophysical Research Letters* 30(20), 2037, doi:[10.1029/2003GL018025](https://doi.org/10.1029/2003GL018025)
- Giacaglia GEO (1980) Transformations of spherical harmonics and applications to geodesy and satellite theory. *Stud Geophys Geod* 24(1):1–11
- Goldstein JD (1984) The effect of coordinate system rotations on spherical harmonic expansions. *J Geophys Res* 89(B6):4413–4418
- Grappo GA (1980) Determination of the Earth's mean equatorial radius and center of mass from Doppler-derived and gravimetric geoid heights. *Manuscr Geod* 5(3/4):201–216
- Heflin M, Argus D, Jefferson D, Webb F, Zumberge J (2002) Comparison of a GPS-defined global reference frame with ITRF2000. *GPS Sol* 6(1/2):72–75
- Heiskanen W, Moritz H (1967) *Physical geodesy*. WH Freeman, San Francisco
- Ilk K-H, Mayer-Gürr T, Feuchtinger M (2005) Gravity field recovery by analysis of short arcs of CHAMP. In: Reigber C, Luhr H, Schwintzer P, Wickert J (eds) *Earth Observation with CHAMP—Results from three years in Orbit*. Springer, Berlin, pp 127–132
- Izsak IG (1964) Tesseral harmonics of the geopotential and corrections to station coordinates. *J Geophys Res* 69(12):2621–2630
- Jeffreys B (1963) Transformation of tesseral harmonics under rotations. *Geophys J R Astron Soc* 10:141–145
- Kaula WM (1961) Analysis of gravitational and geometric aspects of geodetic utilization of satellites. *Geophys J R Astron Soc* 5:104–133
- Kirby JF, Featherstone WE (1997) A study of zero- and first-degree terms in geopotential models in Australia. *Geomat Res Australas* 66:93–108
- Kleusberg A (1980) The similarity transformation of the gravitational potential close to the identity. *Manuscr Geod* 5:241–256
- Kotsakis C (2008) Transforming ellipsoidal heights and geoid undulations between different geodetic reference frames. *J Geod* 82(4/5):249–260
- Lachapelle G, Kouba J (1981) Relationship between terrestrial and satellite Doppler systems. In: Gaposchkin EM, Kolaczek B (eds) *Reference coordinate systems for Earth dynamics*. Reidel, Dordrecht pp. 195–203
- Leick A, van Gelder BHW (1975) On similarity transformations and geodetic network distortions based on Doppler satellite observations. Report No. 235, Department of Geodetic Science, Ohio State University, Columbus
- Lemoine FG, Kenyon SC, Factor JK, Trimmer RG, Pavlis NK, Chinn DS, Cox CM, Klosko SM, Luthcke SB, Torrence MH, Wang YM, Williamson RG, Pavlis EC, Rapp RH, Olson TR (1998) The Development of the Joint NASA GSFC and the National Imagery and Mapping Agency (NIMA) Geopotential Model EGM96. NASA Technical Paper NASA/TP1998206861, Goddard Space Flight Center, Greenbelt, Maryland
- Mayer-Gürr T, Ilk KH, Eicker A, Feuchtinger M (2005) ITG-CHAMP01: a CHAMP gravity field model from short kinematic arcs of a one-year observation period. *J Geod* 78(7/8):462–480
- McCarthy DD, Petit G (eds) (2004) *IERS conventions 2003*. International Earth Rotation and Reference Systems Service (IERS) Technical Note, No. 32, Verlag des Bundesamts für Kartographie und Geodäsie, Frankfurt am Main
- Melbourne W (1983) Project MERIT standards. U.S. Naval Observatory Circular, Report No. 167, Washington, DC
- Pavlis EC (1998) On the reference frames inherent in recent geopotential models. In: Vermeer M, Adam J (eds) *Proceedings of the Second Continental Workshop on the Geoid in Europe*, Budapest, Hungary 10–14, March 1998. Reports of the Finnish Geodetic Institute, Massala 98:4, pp. 29–40
- Pavlis EC (2002) Dynamical determination of origin and scale in the Earth system from satellite laser ranging. *IAG Symposia*, vol 125. Springer, Berlin, Heidelberg, pp 36–41
- Rapp RH (1989) The treatment of permanent tidal effects in the analysis of satellite altimeter data for sea surface topography. *Manuscr Geod* 14(6):368–372
- Rapp RH (1993) *Geometric geodesy (part II)*. Lecture Notes, Department of Geodetic Science and Surveying, Ohio State University, Columbus
- Rapp RH, Rummel R (1976) Comparison of Doppler derived undulations with gravimetric undulations considering the zero-order undulation of the geoid. In: *Proceedings of the First International Geodetic Symposium on Satellite Doppler Positioning*. Defence Mapping Agency, Washington, DC, pp 389–397
- Reigber C, Balmino G, Schwintzer P, Biancale R, Bode A, Lemoine J-M, König R, Loyer S, Neumayer H, Marty J-C, Barthelmes F, Perosanz F, Zhu SY (2002) A high quality global gravity field model from CHAMP GPS tracking data and Accelerometry (EIGEN-1S). *Geophys Res Lett* 29(14). doi:[10.1029/2002GL015064](https://doi.org/10.1029/2002GL015064)
- Reigber C, Balmino G, Schwintzer P, Biancale R, Bode A, Lemoine J-M, König R, Loyer S, Neumayer H, Marty J-C, Barthelmes F, Perosanz F, Zhu SY (2003a) Global gravity field recovery using solely GPS tracking and accelerometer data from CHAMP. *Space Sci Rev* 29:55–66
- Reigber C, Schwintzer P, Neumayer K-H, Barthelmes F, König R, Förste C, Balmino G, Biancale R, Lemoine J-M, Loyer S, Bruinsma S, Perosanz F, Fayard T (2003b) The CHAMP-only Earth gravity field model EIGEN-2. *Adv Space Res* 31(8):1883–1888
- Reigber C, Schmidt R, Flechtner F, König R, Meyer U, Neumayer KH, Schwintzer P, Zhu SY (2005) An Earth gravity field model complete to degree and order 150 from GRACE: EIGEN-GRACE02S. *J Geodyn* 39(1):1–10
- Reigber C, Schwintzer P, Stubenvoll R, Schmidt R, Flechtner F, Meyer U, König R, Neumayer H, Förste C, Barthelmes F, Zhu SY, Balmino G, Biancale R, Lemoine J-M, Meixner H, Raimondo JC (2006) A high resolution global gravity field model combining CHAMP and GRACE satellite mission and surface data: EIGEN-

- CG01C. Scientific Technical Report STR06/07, GeoForschungsZentrum (GFZ), Potsdam
- Schaab H, Groten E (1979) Comparison of geocentric origins of global systems from uniformly distributed data. *Bull Geod* 53(1):11–17
- Schmidt A (1899) Formeln zur transformation der kugelfunctionen bei linearer änderung des coordinatensystems. *Z Math Phys* 44:327–338
- Shkodrov VG (1981) The reference frames and a transformation of the spherical functions. In: Gaposchkin EM, Kolaczek B (eds) Reference coordinate systems for Earth dynamics. Reidel, Dordrecht pp 255–259
- Smith (1998) There is no such thing as ‘the’ EGM96 geoid: subtle points on the use of a global geopotential model. *IGeS Bull* 8:17–28
- Soler T (1998) A compendium of transformation formulas useful in GPS work. *J Geod* 72(7/8):482–490
- Soler T, van Gelder BHW (1987) On differential scale changes and the satellite Doppler system z-shift. *Geophys J R Astr Soc* 91(3):639–656
- Tapley BD, Ries J, Bettadpur S, Chambers D, Cheng M, Condi F, Gunter B, Kang Z, Nagel P, Pastor R, Pekker T, Poole S, Wang F (2005) GGM02—An improved Earth gravity field from GRACE. *J Geod* 79(8):467–478
- Vatrt V (1999) Methodology of testing geopotential models specified in different tide systems. *Stud Geophys Geod* 43(1):73–77
- Weigel G (1993) Geoid undulation computations at Doppler satellite tracking stations. *Manuscr Geod* 18(1):10–25
- West GB (1982) Mean earth ellipsoid determined from SEASAT-1 altimeter observations. *J Geophys Res* 87:5538–5540
- Wigner EP (1959) Group theory and its application to the quantum mechanics of atomic spectra. Academic Press, New York
- Zhu SY, Massmann F-H, Yu YQ, Reigber C (2001) The effect of the geocentric gravitational constant on scale. Scientific Technical Report, 17: 01/12, Geo Forschungs Zentrum, Potsdam